9-30-1991

Deconvolution applications in arterial dynamics

Shanthi Ganesan
New Jersey Institute of Technology

Copyright Warning & Restrictions

The copyright law of the United States (Title 17, United States Code) governs the making of photocopies or other reproductions of copyrighted material.

Under certain conditions specified in the law, libraries and archives are authorized to furnish a photocopy or other reproduction. One of these specified conditions is that the photocopy or reproduction is not to be "used for any purpose other than private study, scholarship, or research." If a, user makes a request for, or later uses, a photocopy or reproduction for purposes in excess of "fair use" that user may be liable for copyright infringement,

This institution reserves the right to refuse to accept a copying order if, in its judgment, fulfillment of the order would involve violation of copyright law.

Please Note: The author retains the copyright while the New Jersey Institute of Technology reserves the right to distribute this thesis or dissertation

Printing note: If you do not wish to print this page, then select "Pages from: first page # to: last page #" on the print dialog screen

Abstract

Title of thesis : **Deconvolution Applications in Arterial Dynamics.**

Shanthi Ganesan

Dr.Peter Engler

Dr.Swamy Laxminarayan

Dr.David Kristol

This thesis deals with the computation of the Arterial Impulse Response Function by deconvolving aortic pressure and flow signals in time domain. Several methods have been developed in the past to obtain a solution for the convolution integral. These are (1) Transform method, and (2) Numerical Approximation methods :
a. Conventional method b. Relaxation methods.

These methods have been applied in the past to the RC network model and it was found to work well. In this thesis, the methods are applied to data from more realistic models and also on data obtained from dogs. The model considered is a 3-element Windkessel model. Studies were conducted in two situations in dogs - one under control situation which is to be compared with the Windkessel model and then under occlusion conditions, with aortic occlusion and occlusion of both carotid arteries.

The parameters of interest in this study of the arterial system in time domain are the total arterial compliance and wave reflections. Reflection studies are made from the impulse response function of the dogs under occlusion conditions.

DECONVOLUTION APPLICATIONS IN ARTERIAL DYNAMICS

by

Shanthi Ganesan

Thesis submitted to the Faculty of the Graduate School of
the New Jersey Institute of Technology in partial fulfilment of
the requirements for the degree of
Master of Science in Biomedical Engineering
1991

APPROVAL SHEET

Title of Thesis: Deconvolution Applications in Arterial Dynamics.

Candidate: Shanthi Ganesan
Master of Science in Biomedical Engineering, 1991.

Thesis and Abstract Approved by the Examining Committee:

Prof. Peter Engler
Associate Professor, Dept. of Electrical Engineering,
NJIT, Newark.

Date

Prof. David Kristol
Director, Dept. of Biomedical Engineering,
NJIT, Newark.

Date

Prof. Swamy Laxminarayan
Program Director of Academic & Research Computing
UMDNJ, Newark.

Date

New Jersey Institute of Technology, Newark, New Jersey.

VITA

Name :

Permanent Address :

Degree to be conferred : Master of Science, 1991
Biomedical Engineering

Date of Birth :

Place of Birth :

Collegiate Institutes Attended	**Dates**	**Degree**
New Jersey Institute Of Technology Newark, NJ 07102.	Sep '89 - Dec '91	Master of Science in Biomedical Engg.
College of Engineering Madras, India.	Oct '84 - May '88	Bachelor of Science in Electrical Engineering

Positions Held	**Date**
Resident Clinical Engineer UMDNJ Newark, NJ.	Jan '90 - May '90
Biomedical Trainee KJ Hospital, Madras, India.	Jan '89 - April '89

ACKNOWLEDGEMENT

I thank Dr.Swamy at UMDNJ for all the help he has rendered to me and all the valuable advice he has given for the successful completion of my thesis. I would like to extend my thanks and appreciation to Dr.Engler and Dr.Kristol at NJIT for the support and encouragement they offered me all the way. I cannot forget the cooperation and the wonderful help rendered by the staff at the Academic Computing Center at UMDNJ and I duly thank them. Finally, I would like to thank my parents, sisters and my good friends for their continuous prayers and encouragement throughout my stay here at NJIT.

TABLE OF CONTENTS

Chapter 1

Introduction

The heart is a pulsatile, 4-chamber pump composed of two atria and two ventricles. The atria pump blood to the ventricles and the ventricles supply the main force that propels blood through the peripheral circulatory system.

The most important feature of the circulation is that it is a continuous circuit Blood flows with almost no resistance in the larger vessels but in the smaller vessels, like arterioles and capillaries, considerable resistance exists. To cause blood to flow through these small "resistance" vessels, the heart pumps blood into the arteries under high pressure - a systolic pressure of 120 mm Hg. The function of the arterial system is to transport blood from the left ventricle to the peripheries.

The large arteries, the aorta in particular, acts as a so-called "Windkessel" [13] [14]. The Windkessel theory is invoked to explain various circulatory phenomena. The volume of blood ejected during systole distends the proximal portion of the aorta and its branches and the elastic energy thus stored in the walls of these vessels is reconverted to energy of flow as the walls recoil in diastole. There is a gradual decline of arterial pressure which would not be seen if the vessels were rigid tubes: in a rigid tube, the pressure would fall abruptly when the pressure at the input to the tube is

abruptly removed. The pressure-flow relationships measured in the ascending aorta offers a very useful means of characterizing the entire arterial tree [1] [25].

Although most physiologic systems are non-linear, assumptions of linearity are often made within certain constraints. The overall properties of the arterial system are non-linear but they are often considered linear, with some justification, over the range of pulse pressure [1] [5]. Such linear approximations not only facilitate mathematical analysis of the system but also provide practical answers.

Since the arterial system is assumed to be linear, linear systems analysis concepts can be applied to characterize the system. Fourier analysis has been applied to characterize the system [21]. The arterial system can be characterized either in the freqeuncy domain by means of its Frequency Response Function (Input Impedance) or in time domain by means of its Time Response Function (Impulse Response Function). The input impedance and the impulse response function are Fourier transform pairs of each other [25].

If p(t) and f(t) are respectively the pressure drop and flow through the system. the system function can be described by the convolution integral in time domain. as given below,

$$p(t) = \int_{-\infty}^{+\infty} f(t-\tau).h(\tau)\,d\tau \tag{1.1}$$

h(t) is the impulse response function.
Fourier transforming to frequency domain yields

$$P(j\omega) = F(j\omega).H(j\omega) \tag{1.2}$$

$H(j\omega)$ is the input impedance and j = $\sqrt{-1}$

The concept of input impedance has proved to be extremely useful in the past in characterizing the systemic circulation [2]. Considerable work has been done in the past in characterizing the arterial system by the systemic input impedance [2] [4] [5]. The input impedance can be calculated by Fourier transforming the measured pressure and flow time histories. The ratio of the modulii of Fourier spectra of pressure and flow yields the modulus of impedance and the difference in phase between those of pressure and flow gives the phase informtion.

The input impedance has the following characteristics. The input impedance at 0 Hz (which is the ratio of mean pressure to mean flow) is the peripheral resistance. At higher frequencies, it approaches the characteristic impedance of the aorta The presence of small minima and maxima in the input impedance is related to wave reflections in the arterial system [33]. Input impedance drops from a value at 0 Hz which is dependent on the peripheral resistance, to a constant value at higher frequencies which is dependent on the capacitive and inductive properties of the aorta, with steepness of the fall dependent on capacitive properties (distensibility) of the aorta. The input impedance is a frequency-dependent quantity, not a time-dependent quantity. In estimating the input impedance by Fourier analysis, the frequency of the phase and modulus spectra is dependent on the heart rate. Only those frequencies that are multiples of the heart rate will contain valid information about the impedance. The first 10 to 20 harmonics are used for computing the input impedance, because the presence of noise at higher frequencies will make the impedance meaningless at these frequencies.

The Impulse Response Function of the arterial system is the time domain description of the system. Both representations are equivalent, but one is in frequency domain (Input Impedance) and the other is in time domain (Impulse Response Function).

The impulse response function is the response resulting from a flow that is a unit impulse function (infinitely short in duration and infinitely high in amplitude with unit area) [3] [6]. In the case of the arterial system, application of these excitations is not desirable, though this method of estimating impulse response function has been examined before [3]. So, we make use of the heart as a pump and resort to determining h(t) from the measured pressure drop p(t) and flow f(t) through the arterial system.

Impulse response function computations have been recently studied [3] [6] [23] [31]. The Impulse response function has clinical significance and can be used in the derivation of the transfer function of a diseased segment of the artery. Since the impulse response function (IRF) is computed from pressures and flows with repetition frequency of the heart rate, it is not the result of a single impulse of flow but is repeated with the heart rate. The arterial system characterization in time domain is easily merged with the time domain characterizations of the left ventricle for the study of LV-SA (left ventricle/Systemic arterial system) interactions [7] [23]. It also appears conceptually easier that the IRF is a single graph whereas the input impedance consists of 2 sub-plots - the modulus and phase spectrum.

The impulse response function emphasizes arterial compliance. For the case of a Windkessel model which mimics the arterial system under control conditions [4] [14],

the impulse response function (for a periodic excitation of the model with period T) is given by:

$$h(t) = R_c\delta(t) + \exp(-t/\tau)/(C(1-\exp(-T/\tau)) \qquad (1.3)$$

The model consists of a resistance R_c (equal to the characteristic impedance of the arterial system), R_p (representing the peripheral resistance of the arterial system) and a capacitor C (representing the total arterial compliance). $\delta(t)$ is the Dirac Delta function and τ is the time constant given by $\tau = R_p.C$.

The therotical IRF of the Windkessel model consists of a delta function and an exponentially decaying function with time constant τ. When pressure-flow relations in the arterial system can be approximated with the Windkessel model, the total arterial compliance can be obtained by estimating the height of the exponential decay in the impulse response function, extrapolated to time zero [6]. The decay time of this exponential is the same as that of the diastolic part of aortic presure tracing. Also, a reflection site manifests itself as a peak in the IRF. The information on reflections is therefore directly apparent. The major reflection points in the arterial system can be located in time domain analysis. The pattern in time domain analysis becomes less complicated if we match the source to the characteristic impedance of the ascending aorta. This analysis is called time domain reflectometry [27].

The impulse response function can be computed either directly by deconvolving the pressure and flow time histories or indirectly by Fourier transforming the input impedance. This indirect method of computing the IRF of the arterial system has been investigated perviously [6]. The limitation of this indirect transform process for obtaining the IRF from the input impedance, is that the transformation involves an infinite integral , the evaluation of which requires a knowledge of the input impedance

for all frequencies upto ∞. The amplitudes of the harmonics of pressure and flow decrease with frequency and will gradually disappear in the noise after the 10^{th} to 20^{th} harmonic. For these frequencies the impedance cannot be calculated. But the input impedance at higher frequencies approaches the characteristic impedance of the aorta and does not reach zero values. If this truncated impedance is transformed, its effects are reflected as oscillations that are superimposed on the actual impulse response function. So, before transformation of the impedance data to time domain can be performed, the Dolph- Chebyshev filter was used to minimize the truncation effects.

The procedure for calculating the IRF by the direct method involves finding an acceptable solution to the convolution integral, ie. eq. 1.1. This is a very complex issue and requires numerical approximation methods. Numerical techniques have been applied in the past and used as an analytical tool in the study of biological systems [9] [10]. A number of algorithms have been developed in the past to compute the IRF using numerical approximation methods [8].

These numerical methods include

1. Conventional method.
2. Iterative methods
    a. Jacobi's method.
    b. Relaxation methods
    c. Modified or Epsilon method.

In the past, these methods have been applied on simple R-C network models only [8] and they have been found to work fairly accurately on these simple models. It

was found that these methods were sensitive to the start point of deconvolution, the sampling rate and the relaxation parameter, α in the case of the relaxation methods. The start point plays a critical role in the accurate estimation of the IRF as the input value at t = 0 can never be zero. The sample rate should also be chosen such that the sampling interval is not large as it will increase the error in the IRF. To acquire meaningful IRF's, these parameters have to be chosen properly.

The objective of the proposed work is to extend these numerical analysis methods to compute the impulse response function of more realistic models which mimic the real-life situation. The 3-element Windkessel model serves as a good model of the arterial system under control conditions. Data generated from this model are analyzed and the various deconvolution procedures are applied to this data to compute the IRF of the windkessel model. A proper choice of start point, sample rate and the relaxation parameter α have to be made in order to get meaningful impulse response functions.

Then the numerical methods are applied to the pressure and flow measurements obtained in the dog. Impulse response functions are computed for the following situations.

1. Control animal.
2. Occlusions of the aorta at the level of the diaphragm.
3. Occlusion of both carotid arteries.

Reflection studies are made from the impulse response functions of the dog under occlusion conditions.

These studies are performed with particular emphasis on the effects of sample rate, the start point and the relaxation parameter α on the computation of the impulse response function.

Chapter 2

Review of Mathematical Methods

The work done in the thesis utilizes several mathematical methods already developed in a previous study [8]. This chapter briefly reviews these various methodologies.

The impulse response function can be calculated either directly by deconvolving the equation

$$p(t) = \int_0^t f(t-\tau).h(\tau)d\tau \tag{2.1}$$

or by inverse fourier transforming the input impedance into its time domain counterpart.

$$h(t) = \sum_0^\infty H(j\omega).\exp(j\omega t)d\omega \tag{2.2}$$

The input impedance and impulse response function are Fourier transform pairs of each other.

2.1 Transform method

The indirect or transform method of computing the impulse response function has been investigated previously [6]. This method of computing the Impulse response function has a major problem. The above equation shows that the input impedance values should be known for all frequencies upto infinity, while in practice, only a lim-

ited number of harmonics can be calculated. It is not possible to compute H(jω) for frequencies above 40 Hz. This is because above this frequency range, noise in the data makes it meaningless to compute H(jω). The input impedance has to be truncated at some finite frequency. If the input impedance reached steady-state zero values at the cut-off frequency, then the inverse transformation would yield meaningful results. But in the case of the arterial system, the input impedance approaches the characteristic impedance at higher frequencies and does not reach zero values. The transformation of the truncated input impedance at some cut-off frequency implies the presence of a mathematical window. The effects of such a window or filter appear as oscillations superimposed on the actual impulse response function. Therefore, before transformation of the input impedance data, some form of frequency domain smoothing has to be applied. The Dolph-Chebyshev filter [29] has been used to minimize the effects of truncation in order to get meaningful results [6].

Though this method of using a filter is a good solution under control conditions, it may not be efficient when reflections are present Reflections manifest themselves as peaks in the impulse response function. But when frequency domain smoothing is applied, important information may be lost. This is specially true when the amplitude of these reflection peaks are small compared to the initial delta function in the IRF plot.

2.2 Direct methods

The more efficient way of calculating the IRF would be the straight-forward method of subjecting the measured pressure and flow data to a deconvolution procedure. However, the procedure of deconvolution is very complex. This method is very sensitive to the presence of noise in the data and the initial value of the excitation time

history is critical in the computational procedures. Various numerical approximation methods have been developed in the past for deconvolution with emphasis on the arterial system [8]. In the following section, the various deconvolution procedures are described and the method which yielded the best results is described in greater detail.

The direct method of computing the impulse response function involves the deconvolution procedure. Numerical methods have to be applied to solve the convolution integral.

$$p(t) = \int_0^t f(t-\tau).h(\tau)d\tau \tag{2.3}$$

where h(t) is the impulse response function, p(t) is the pressure drop across the arterial system and f(t) is the flow through the system. Our objective is to calculate h(t), by deconvolution, knowing f(t) and p(t).

The various methods used are :-

1. Conventional method
2. Iterative methods.

2.2.1 Conventional method

In the Conventional method, the Convolution integral is expressed as a discrete summation.

$p_x = \sum_{y=0}^{x} f_(x-y).h_y\Delta t$ (2.4)

where x = 0, 1, 2....n.

This can be written as a system of equations.

$p_0 = f_0 h_0 \Delta t$

$p_1 = (f_1 h_0 + f_0 h_1)\Delta t$

$p_2 = (f_2 h_0 + f_1 h_1 + f_0 h_2)\Delta t$

.

.

.

$$p_n = (f_n h_0 + f_{n-1} h_1 + ...+ f_0 h_n)\Delta t \quad (2.5)$$

Writing this in matrix form and solving for the impulse response function vector H, we get the general form

$$h_x = (1/f_{xx})(p_x/\Delta t - \sum_{y=0}^{x-1} f_{xy} h_y) \quad (2.6)$$

where x = 0,1,2....n.

Effectively we are seeking a solution for: $F \times H \times \Delta t = P$

where F is the flow matrix, P is the pressure matrix and H is the impulse response function matrix. The conventional method is highly sensitive to errors present in the data points [8] [9]. The sampling interval Δt has also a very significant influence. Increasing the sampling interval will increase the error in the IRF The input value at t = 0 is also an important factor. In the case of the arterial system the initial aortic flow values are 0 or near-zero values. So, the start point of deconvolution plays a critical role in the estimation of the impulse response function.

2.2.2 Iterative methods

Iterative procedures can be applied to solve equations of the type $F \times H = P$ The iterative methods are numerical methods that start from any initial guess H_0 and can produce an improved approximation H_{k+1} from the previous approximation H_k that can be terminated at will.

In our case,

$$P = F \times H \times \Delta t \quad (2.7)$$

This can be written in matrix form. P is the pressure matrix, F is the flow matrix

and H is the impulse response function matrix. We can split the matrix F into M and N such that F = M-N.

Therefore eq. 2.7 can be written as

$P = (M\text{-}N)H\Delta t$

$MH = NH + P/\Delta t.$

A successful splitting satisfies two different requirements.

a. The new vector H^{k+1} should be easy to compute. Hence M should be a simple and invertible matrix.

b. The sequence H^k should converge to the true solution H. The choice of M is crucial in numerical analysis [11] [12].

Jacobi's method

The Jacobi's method is an example of "simultaneous displacements". At the end of each iteration, we replace all the elements of H^k simultaneously with the elements of H^{k+1}. This method is also very sensitive to the start point of deconvolution.

Gauss-Seidal method

A better method would be to start using each component of the new vector H^{k+1} as soon as it is computed ie. H^{k+1} takes the place of H^k at a time. Thus H^k can be destroyed as fast as H^{k+1} is created. This requires only half as much storage. If we use the computed values as soon as we have calculated them , we have a method of successive displacements referrred to as the Gauss-seidal method [12] [28].

Relaxation methods

The method used for numerical approximation should be such that it converges to the true solution quickly. To make it converge even faster than the Jacobi and Gauss-seidal method, we introduce a relaxation factor α to move closer to the solution. This factor is called the relaxation parameter.

We get the general form for the impulse response function vector H,

$$h_x^{k+1} = h_x^k + (\alpha/f_{xx})(p_x/\Delta t - \sum_{y=0}^{x-1} f_{xy} h_y^{k+1} - \sum_{y=x}^{n} f_{xy} h_y^k) \quad (2.8)$$

where x = 0, 1, 2....n.

The parameter that plays a critical role in this method is the relaxation parameter α. When $\alpha = 1$, this method reduces to the Gauss-Seidal method. If $\alpha > 1$, it is called succesive over-relaxation and if $\alpha < 1$, it is called under-relaxation.

2.3 Relaxation method

This numerical method for solving the convolution integral is found to be very useful. The IRF is dependent on the value of the relaxation parameter α. This α plays a critical role in the convergence of the deconvolution solution. Depending on the value of α, it reduces to either the Gauss-Seidal method or the under-relaxation or the over-relaxation method. The relaxation method has been applied to the excitation and response data generated by the RC network model [8]. The parameters that were found to influence the accuracy of the impulse response function computed by the relaxation methods are

1. The relaxation parameter
2. The start point

3. The number of iterations

The relaxation parameter α has a very strong influence in the accurate estimation of the IRF. As the value of α is varied, it gives grossly different results. It was found that the under-relaxation method with values of α between 0.1 - 0.5 gave best results for the RC network model. Over-relaxation method resulted in totally incongruous IRF's [8].

The start point was also an important factor in the accurate estimation of the impulse response function. In the case of the arterial system, the initial value of the input time history assumes zero or near-zero values. But this method requires the initial flow value to be a non-zero value. The effect of selecting the next non-zero value as the start point can give rise to serious errors in the computation of the IRF, especially if noise is present in the data.

The number of iterations does not affect the solution after it has converged. It is variable only to a point where the final solution is reached.

So, this relaxation method has been used to compute the IRF of the systemic arterial tree of the dog from the measured pressure and flow data, after careful checks of the method on a model of the arterial tree.

The methods described above have been applied to the excitation and response data from the Windkessel model, the pressure and flow data from dogs, both under control conditions and under occlusion conditions and are reported in the subsequent chapters.

Chapter 3

Model Studies

3.1 Windkessel model

Linear mechanical and electrical models are so often used in circulatory physiology When properly used, such models are important to the understanding and quantification of the cardiovascular system. The chosen model must be one minimally necessary to describe system behavior. There should be a one-to-one correspondance between various model elements and system components.

The Windkessel model is an electrical model of the arterial system under control conditions. Using this model , we can simulate the functions of the arterial tree under normal conditions. This model is a good approximation of the input impedance of the systemic arterial tree under control conditions [13]. The original Windkessel model formulated by Frank, was modified by Westerhof who combined the original windkessel model and the characteristic impedance of the aorta [14]. The electrical circuit is given in figure (1). The 3-element Windkessel model consists of a resistor R_c (equal to the characteristic impedance of the aorta) in series with a parallel arrangement of another resistor R_p (equal to the peripheral resistance of the arterial system) and a capacitor C (total arterial compliance).

The values of the components used in this model are R_p = 20K, C = 60μF and R_c = 1.2K. The time constant for this model is given by $\tau = R_p.C = 1.2$ secs.
The excitation (input) f(t) and the response (output) p(t) time histories are given in figure (2).

The input impedance for this model as a function of frequency is

$$H(j\omega) = R_c + (1/C) \cdot (1/(j\omega+1/\tau)) \tag{3.1}$$

where $\omega = 2\pi f$ and f is the frequency.
The input impedance calculated for the windkessel model by inverse Fourier transforming the pressure and flow time values can be seen in figure (3).

The impulse response function of the model can be obtained by the transformation of eq. 3.1 to time domain.

So,

$$h(t) = R_c\delta(t) + (1/C)\exp(-t/\tau) \tag{3.2}$$

where $\delta(t)$ is the delta function.

For a periodic excitation T on the model, we get

$$h(t) = R_c\delta(t) + \exp(-t/T)/(C(1-\exp(-T/\tau)) \tag{3.3}$$

From eq. 3.3, it can be seen that the theoretical impulse response function of the 3-element windkessel model consists of a delta function $\delta(t)$ and an exponentially decaying function with time constant τ. The impulse response function shows an initial sharp peak and then an exponential decay. The height of the exponential decay extrapolated to time 0 (using T and τ) gives total arterial compliance C [6].

3.2 Parameters of interest

The various parameters that are of interest in the study of arterial hemodynamics are peripheral resistance, characteristic impedance, arterial compliance and arterial reflections [1] [18] [30] [32].

Impedance is the measure of the opposition to the flow presented by a system. Impedance cannot be defined as "instantaneous impedance" because it is a frequency-dependent quantity [18]. At any one time, pressure depends not only on flow at the same instant but also on flow at previous instants. Input impedance is the ratio of pressure and flow at a particular arterial site which may be regarded as input to all the vascular tree beyond this site.

Characteristic impedance is the ratio of pressure to flow in an artery when not influenced by wave reflections which would be an artery of infinite length. Peripheral resistance is the input impedance of the arterial tree at 0 Hz Characteristic impedance is the input impedance at frequencies higher than 5 Hz where fluctuations caused by reflections have settled [30].

Arterial Compliance can be defined as the ratio of the increase in volume to the increase in pressure. It gives a measure of the total quantity of blood that can be stored in a given portion of the circulation. The greater the compliance of the arterial system, the lower will be the rise in pressure for a given stroke volume of blood pumped into the arteries.

Various techniques are available for computing the total arterial compliance. In

the past, compliance has been estimated by analyzing the arterial pressure waveform in which the diastolic pressure decays with a time constant that is a product of total arterial resistance and compliance [15] [16]. Almost all existing methods of estimating compliance assume that the arterial pressure-volume relationships is linear ie. compliance is constant and not pressure-dependent.

When the pressure-flow relations in the arterial system can be approximated with a windkessel model, it has been shown that the exponential portion of the impulse response function can be utilized in estimating the total arterial compliance [6]. Since the impulse response function and the input impedance are Fourier transform pairs, the arterial compliance can be determined from the impedance function. The concept of frequency response vector diagrams was used to estimate compliance from the frequency-dependent input impedance [17].

Reflected waves are present whenever there is a change in the characteristic impedance of the flow pathway. Since this occurs at almost every point of branching in the vascular tree, reflected waves exist to some extent throughout the circulation. Possible reflecting sites include branching points, areas of alteration in arterial distensibility and high-resistance arterioles. The existence of wave reflections is determined by various observations [18] [26] [27].

1. The shapes of the pressure and flow waves measured in the ascending aorta are different.
2. During ventricular ejection, the aortic pressure may continue to increase while the flow is decreasing.
3. The amplitude of the pressure pulse increases as it travels towards the periphery.

When reflected waves are present, the observed pressures are a combination of incident and reflected waves and also for flow. Pressure and flow waves contain both incident and reflected components. The presence of arterial wave reflections may be inferred from characteristic alterations in the pressure pulse as it propogates along the aorta. Both the magnitude and timing of the reflected waves are important in assessing potential physiologic significance. Since a reflected pressure wave adds to the forward wave, a wave returning during systole would decrease ventricular afterload. Reflected flow waves however, subtract from the forward flow pulse. Therefore, a wave returning during systole diminishes forward flow and is disadvantageous to ventricular ejection [18] [27].

The two descriptions of the arterial system, Input Impedance and Impulse response function are equivalent characterizations of the system. They contain the same information since they are derived from the same signals, pressure and flow. However, each characterization emphasizes different aspects of the arterial tree. The frequency domain characterization emphasizes the peripheral resistance and characteristic impedance. The time domain characterization emphasizes arterial compliance and reflections. Arterial reflections show up as distinct peaks in the IRF [3] [6].

3.3 Results

3.3.1 IRF calculation by transform method

As the input impedance and the impulse response function are Fourier transform pairs of each other, we can obtain the IRF by inverse Fourier transforming the input impedance which is given by

$$\mathrm{H}(\mathrm{j}\omega) = P(j\omega)/F(j\omega) \tag{3.4}$$

The limitation of the Fourier transform process for obtaining the impulse response function from the input impedance is that the transformation involves an infinite integral the evaluation of which requires a knowledge of H(jω) for all values of ω upto infinity. Truncation of H(jω) is valid provided the values of H(jω) have reached steady-state zero values at the cut-off frequency. However the impedance values at higher frequencies approximate the characteristic impedance and never reaches zero values. Transformation of such a function implies the presence of a mathematical window, the effects of which are manifested as oscillations superimposed on the resulting IRF. In order to eliminate these truncation effects, the approach taken is to filter the higher harmonics so that the amplitudes at these higher harmonics taper off to negligible values. The filter that was used to smoothen the IRF was the Dolph-Chebyshev filter, based on the Chebyshev polynomial [6] [28] [29]. The IRF of a Windkessel model computed by the transform method is illustrated in Fig (4).

Without filter

The impulse response function is computed by inverse Fourier transforming the input impedance. The input impedance is first computed by using the "pressure" and "flow" values from the Windkessel model. The input impedance is truncated to a finite number of frequencies before transformation. The oscillations superimposed on the IRF are seen in Fig (4).

With Dolph-Chebyshev filter

Before transformation of the input impedance data to the time domain can be performed, a suitable filter was chosen to minimize the effects of truncation. A Dolph-Chebyshev filter was used as a filter. As shown in earlier works [6], this has proved

to be very effective in eliminating the spurious oscillations. The filter effects are illustrated in Fig (4).

3.3.2 IRF calculation by direct methods

Conventional method

The Conventional method was first employed to compute the impulse response function. The start point of deconvolution had to be carefully selected since the initial values of flow are 0 or nearly 0.

The start point of deconvolution was first described in terms of the heart period T. In the windkessel model, the heart period was 0.99 secs. Initially the start point was set to correspond to a time point of t = 0.4 secs located in the rising segment of the systolic part of the pressure waveform. The IRF did not exhibit an exponential decay. Various other start points were considered but no improvements were achieved. An example of the computed results is shown in Fig (5a) & Fig (5b).

Gauss-Seidal method

The Windkessel data were then analyzed using the Gauss-Seidal method. The computed IRF did not resemble realistic results. This is illustrated in Fig (5c) & Fig (5d).

Relaxation method

Relaxation method is an iterative procedure. This method introduces a relaxation parameter α to control the stability of the iterative solution of the deconvolution Proper choice of α is the key to the successful application of the method.

When $\alpha > 1$, ie. over-relaxation, it was not possible to retrieve the IRF from the "pressure" and "flow" data from the windkessel model as can be seen in Fig (6).

The Under-relaxation method was next tried with the relaxation parameter $\alpha < 1$. The relaxation parameter was first chosen to be = 0.01. The impulse response function was computed when deconvolution was initiated at different start times. The IRF plots are shown in Fig (7a). The impulse response function is composed of an initial peak followed by an exponential decay. The compliance value was calculated by extrapolating the exponential part of the IRF to time t = 0.

Then the relaxation parameter was varied from 0.02 to 0.09 and the impulse response functions were computed for different start times. The compliance was estimated from the plots for the different parameters and the results are tabulated. The impulse response function plots are shown in Fig (7) & Fig (8). The tabulated results are shown in the next page.

Table 3.1: Under-relaxation method. Sample rate - 100 samples/sec.
Model Compliance = 60 μF

Alpha	Start time secs	Compliance ($\times 10^{-6}$) $gm^{-1}.cm^4.sec^2$
0.01	0.4	very high
	0.45	
	0.5	308
0.02	0.40	222
	0.45	216
	0.5	160
0.04	0.50	86
	0.52	65
	0.53	56
0.05	0.50	117
	0.51	62
	0.52	54
0.06	0.49	68
	0.50	62
	0.51	54
0.07	0.48	66.3
	0.49	60
	0.50	56
0.08	0.47	66
	0.48	60
	0.49	50
0.09	0.46	66
	0.47	61
	0.48	56

It was seen that the value of alpha plays a very important part in the accurate estimation of the IRF. Values of α greater than 0.05 gave meaningful results. The IRF plot manifested an initial peak as expected followed by an exponential decay. The best results in terms of α and start point are tabulated as follows. The compliance of the Windkessel model (Fig 1) was 60 $(\times 10^{-6})$ $gm^{-1}.cm^4.sec^2$.

Table 3.2: Results

Alpha	Start time secs	Compliance $(\times 10^{-6})$ $gm^{-1}.cm^4.sec^2$
0.05	0.51	62
0.06	0.50	62
0.07	0.49	60
0.08	0.48	60
0.09	0.47	61

The relationship between α and start time is shown in Fig (14a). It was found that as alpha was increased from 0.01 to 0.09, the start times of deconvolution at which the impulse response function plots gave good estimates of compliance (in accordance with the model value) was found to decrease.

Calculation of the IRF is very dependent on the start time . Small variations in the start time resulted in large changes in the impulse response function. Start times, approximately about 0.47 - 0.5 secs gave exact values of compliance in accordance with the capacitor element in the model, C = 60 ($\times 10^{-6}$) $gm^{-1}.cm^4.sec^2$.

The **start time** can be described physically with respect to pressure and flow data values in time domain. The flow values are very critical in computing the IRF since the initial values of flow are 0 or nearly 0. ie, at the beginning of the heart period, the flow is not much but rises to a peak towards the middle of the heart period T.

The pressure and flow values exhibit characteristic shapes. Ascending aortic flow is essentially zero throughout the later stages of diastole. When the aortic valve opens, a rapid increase in flow is observed that reaches a peak prior to the midpoint of the period of ejection and then rapidly decreases to the point where the aortic valve closes. A brief period of backflow followed by several low-magnitude oscillations, is present during early diastole. Aortic blood pressure rises rapidly at the onset of ejection as blood moves into the aorta from the left ventricle and peak pressure is attained shortly after peak flow occurs. Pressure then decreases rapidly until the aortic valve closes, at which time a deflection called a dicrotic notch is recorded. During diastole the aortic pressure continues to decrease as blood continues to move from the aorta into the peripheral vasculature.

The **sample rate** is another factor which has an effect on the computation of the IRF. "Pressure" and "flow" data values from the windkessel model were interpolated using the software "SIGNA" to obtain a sample rate of 256 samples/sec.

The Impulse Response Function was computed by the direct methods. The Conventional method was first tried with this new sample rate of 256 samples/sec. The computed IRF is shown in Fig (9a). This method was not successful in extracting the IRF from the excitation and response data.

The Gauss-Seidal method and the Over-relaxation method were also tried as illustrated in Fig (9b) & Fig (10). These methods of deconvolution also proved futile in recovering the IRF.

The Under-Relaxation method was next tried with the relaxation parameter α set to be = 0.01. The Impulse Response Function plots obtained using this method is shown in Fig (11a). The data of Figs (11 - 13) was computed at a sample rate of 256 samples/sec. The plot follows a negative exponential curve after the initial peak. The start point or start time of deconvolution is a very important parameter in the accurate estimation of the IRF. As the start time is varied from 0.54 - 0.55 secs, there is a shift in the IRF plot, though the curves follow a general pattern. The compliance values were estimated by extrapolating the exponential decay to time zero for all the three cases. It was found that when the start time was equal to 0.55 secs (which corresponds to a start point of deconvolution of 141 samples), the estimated compliance from the IRF plot was found to be 58 ($\times 10^{-6}$) gm^{-1}. $cm^4.sec^2$). The value closely agrees with the value of the capacitore in the Windkessel model - C = 60 ($\times 10^{-6}$) $gm^{-1}.cm^4$ $.sec^2$. It was observed that the values of estimated compliance decreased as the start times were increased.

Then the Under-Relaxation method was repeated with α = 0.02. Start time t = 0.51 secs corresponding to a start point of 132 samples gave a good estimate of the

compliance. Estimated compliance from the IRF plot = 59.3 ($\times 10^{-6}$) $gm^{-1}.cm^4.sec^2$.

The relaxation parameter α was then made equal to 0.03 and the start times of 0.48 secs, 0.49 secs & 0.5 secs were considered. When the start time was made equal to 0.49 secs, the IRF plot gave a good estimate of compliance. This is shown in Fig (11c).

As the values of α are increased from 0.01 to 0.03, the start times of deconvolution at which the impulse response function curves gave good estimates of compliance were found to decrease. The results are tabulated in Table 3.3:

Table 3.3 Under-Relaxation method. Sample rate = 256 /sec.

Alpha	Start time secs	Compliance ($\times 10^{-6}$) $gm^{-1}.cm^4.sec^2$
0.01	0.545 0.55	64.28 58.4
0.02	0.51 0.515 0.52	62.7 59.3 56
0.03	0.48 0.49 0.50	63.96 60 53.94
0.04	0.45 0.46 0.47	67.2 62.6 58.8

Table 3.3 Under-Relaxation method. Sample rate = 256/sec.

Alpha	Start time secs	Compliance ($\times 10^{-6}$) $gm^{-1}.cm^4.sec^2$
0.05	0.44	65
	0.45	61.3
	0.46	55.5
0.06	0.44	60.3
	0.45	57
0.07	0.43	62
	0.44	57.3
0.08	0.41	64
	0.42	60.3
0.09	0.41	63.9
	0.42	59

The relaxation parameter was then made equal to 0.1 and the impulse response function was computed for different start times of deconvolution. The IRF plots are shown in Fig (13b). It was seen that the plots had an initial peak followed by an exponential decay. The compliance was computed from the plots by extrapolating the exponential decay to time zero. A start time of t = 0.41 secs gave good results.

The relationship between α and the start time of deconvolution is seen in Fig (14b).

As was the case when the sample rate was 100 samples/sec, as α was increased, the start times of deconvolution at which the IRF plots gave good estimates of compliance was found to decrease.

Chapter 4

Animal Studies

The deconvolution methods are now applied to flow and pressure measurements made in dogs. The experimental protocols for obtaining the pressure and flow data under various physiological conditions are detailed in [6]. Studies were conducted in two situations. The first situation is the control condition. This situation is to be compared with the Windkessel model. The second situation is under occlusion condition when the aorta and the carotid arteries are occluded. Reflection studies are made during these occlusion conditions.

4.1 Control Situation

The impulse response function of the arterial system of a dog were computed and analyzed using the deconvolution methods. Three different heart rates were considered. The three cases were labelled as doghr1, doghr2 & doghr3. The heart rates were respectively 32 beats/min, 85 beats/min & 129 beats/min and all the data were sampled at 200 samples/sec. The flow and pressure waveforms measured in the aorta of the dog with heart rate 85 beats/min are shown in Fig (15).

Table 4.1: Hemodynamic Parameters.

Dog	R_p $(\times 10^3)$ gm.cm^{-4}.sec^{-2}	C $(\times 10^{-6})$ gm^{-1}.cm^4.sec^2	τ secs
Doghr1	8.8087	364	2.941
Doghr2	7.446	312	2.324
Doghr3	7.542	307.6	2.32

4.2 Results

The arterial impulse response function was computed using all the methods discussed in the previous sections.

4.2.1 IRF calculation by transform method

In the transform method, the input impedance of the arterial system of the dog under different heart rate conditions were first calculated by subjecting the flow and pressure time data to Fourier transformation. The modulus and phase of the input impedance for the three cases considered are shown in Fig (16). The peripheral resistance, R_p was calculated from the input impedance plot by using the value of the input impedance at 0 Hz. The arterial compliance was calculated by fitting an exponential to the diastolic portion of the pressure curve From the decay time of the exponential portion of the diastolic pressure tracing, the time constant τ was found. From a knowledge of τ and R_p, the total arterial compliance is given by $C = \tau/R_p$.

The impulse response function was then calculated by inverse Fourier transforming the input impedance using the method designed in [6]. One of the great drawbacks of the transform method arises from the fact that the input impedance is an infinite function. The values of input impedance at higher frequencies approaches the characteristic impedance of the aorta and never reaches steady zero values. The data therefore needs to be truncated at some finite frequency, a process which obviously gives rise to large oscillations superimposed on the computed IRF. This is illustrated in Fig (17). In order to eliminate these oscillations, the method requires some form of frequency domain smoothing. A smoothing function that has shown to be very effective in eliminating the oscillations is the modified version of the Dolph-Chebyshev function as shown in [6]. The effect of using these filters in computing the IRF is illustrated in Fig (17a), (17b) & (17c). The total arterial compliance was estimated from the impulse response function plot by extrapolating the exponential decay to time zero (after correction of the periodic excitation T).

4.2.2 IRF calculation by direct methods

The emphasis of the work done in this thesis is on the application of direct methods of evaluating the arterial impulse response function. Several methods have been investigated starting from the basic conventional approach of deconvolution of pressure and flow time histories.

Conventional method

In the Conventional method, the pressure and flow data were subjected to a direct deconvolution procedure using eq. 2.6. One of the critical aspects of this method is the appropriate choice of the starting point for initiating the deconvolution process.

As flow values are near-zero during the initial part of the curve, several start points were chosen beginning from the first non-zero values. None of these choices provided a satisfactory impulse response function. Examples of computed IRF's for the three cases for start times of t = 0.2 secs, 0.225 secs & 0.25 secs are illustrated in Fig (18a), (18b) & (18c).

Gauss Seidal method

Mathematical procedures for computing the IRF using Numerical analysis methods are detailed in previous sections. By varying the relaxation parameter the system of equations can be made to provide stability to the solutions of equations. When the relaxation parameter is kept unity, the procedure becomes the Gauss-Seidal method.

This method was applied to compute the IRF of the arterial system of the dog data. The initial start times were again varied to determine if an optimum value existed. However, it was not possibe to derive meaningful impulse response functions from the pressure and flow time histories using this method. Fig (19) illustrates the computed impulse response functions for various start times.

Over-Relaxation method

The relaxation procedures described in chapter 2 were then applied by chosing the relaxation parameter α to be greater than 1, thus making the system over-relaxed. Neither the various start times nor the increase in α were able to provide meaningful estimates of the IRF. The results are shown in Fig (20) & Fig (21).

Under-Relaxation method

In contrast to the Over-relaxation methods, the under-relaxation procedure assumes values for α to be less then unity. This method was then used to compute the IRF from the flow and pressure values. The relaxation parameter was first chosen to be 0.01. The start times were varied between 0.3 - 0.325 secs. The IRF plot is shown in Fig (22a). The compliance value was estimated by extrapolating the exponential part to time zero (after correction of the periodic excitation T). The compliance of the arterial system of doghr1 was first computed from the diastolic pressure decay and the time constant τ and is found to be 364 $(\times 10^{-6})\mathrm{gm}^{-1}.\mathrm{cm}^4.\mathrm{sec}^2$. The compliance value which closely matched this actual compliance value was when the start time of deconvolution was chosen to be 0.33 secs. This corresponded to a start point of the 66th sample. It was observed that as the start times were increased, the values of compliance decreases.

The same relaxation parameter of 0.01 was then used to compute the IRF of the arterial system of doghr2. Different start times were used to compute the IRF. When deconvolution was initiated at 0.32 secs, the compliance estimated from the IRF plot matched closely with the total arterial compliance estimated from the diastolic pressure decay, as shown in Fig (23a). Again, α was taken to be 0.01 and the under-relaxation method was used to compute the impulse response function of doghr3.

Then, the relaxation parameter was changed to 0.02 & 0.03. The impulse response functions of doghr1, doghr2 and doghr3 were computed. The IRF plots are seen in Figs (22), (23) & (24).

Table 4.2: Under-Relaxation method

Dog	Alpha	Start time secs	Estimated Compliance ($\times 10^{-6}$) $gm^{-1}.cm^4.sec^2$	Compliance estimated from exponential fit method
Doghr1	0.01	0.325	433	
		0.33	358	
		0.335	331	
	0.02	0.29	414	364
		0.295	377	
		0.3	352	
	0.03	0.285	340	
		0.29	313	
		0.3	264	
Doghr2	0.01	0.31	497	
		0.32	350	
		0.325	283	
	0.02	0.3	378	312
		0.305	326	
		0.31	293	
	0.03	0.295	331	
		0.3	327	
Doghr3	0.01	0.275	339	
		0.28	307	
		0.29	290	
	0.02	0.25	560	307
		0.26	307	
		0.265	284	
	0.03	0.24	367	
		0.245	360	
		0.25	242	

The results indicated that a relationship seemed to exist between α and the times at which deconvolution was initiated. It was seen that as the relaxation parameter α was increased, the optimum start times yielding good estimates of compliance were found to decrease. This was observed for all three cases.

This is illustrated in Fig (25).

4.3 Occlusion conditions

Reflection Phenomena

In cardiovascular dynamics, it is well known that the pressure and flow waves are not purely waves travelling outwards from the heart, but they include a number of relections from bifurcations. All waves generated by the heart are partially reflected at many bifurcations [18].

The presence of wave reflection within the arterial system is demonstrated by two phenomena, (1) the amplification of pressure waves in some large arteries, particularly the aorta, (2) the different shapes of pressure and flow in the ascending aorta. The viscous properties of fluid would make the amplitude of pressure waves diminish continuously as they travel out into the arterial tree [18]. But the pressure pulse increases in amplitude along the aorta. This means that reinforcement by reflected waves in the distal aorta outweighs viscous damping. The shape of the aortic flow pulse indicates the presence of reflections, because in their absence, the waveforms of pressure and flow would be almost identical. But the waveforms of pressure and flow

are quite different as can be seen in Fig (15). Sustained pressure during ejection and diastole are due to reflected waves from the periphery [24].

Reflections are generated in a vascular system whenever there is a "mismatching" of impedances. Impedance is a frequency-dependent quantity determined by the ratio of pressure to flow. Significant changes of impedance can occur in the course of normal physiological adjustments of the circulation.

In as much as the input impedance and the impulse response function are equivalent descriptions, some aspects of the system are enhanced better by one than the other. The reflection phenomenon is a characteristic that is seen as peaks in the input impedance [2] [18] [30]. The IRF is capable of bringing out the reflections better than the input impedance can. However, computation of the impulse response function by the inverse transformation and using the frequency domain filtering procedure tends to obscure the reflection peaks due to mathematical smoothing. Direct deconvolution methods are therefore most preferable if it can be achieved. In order to study these reflection pheneomena, impulse response functions were computed for the following situations.

(1) When aorta was occluded at the level of the diaphragm and

(2) During occlusion of both carotid arteries.

The hemodynamic parameters of the dogs, under occlusion conditions are in the table below:

Table 4.3. Hemodynamic Parameters

Dog	R_p $(\times 10^3)$ gm.cm^{-4}.sec^{-2}	C $(\times 10^{-6})$ gm^{-1}. cm^4.sec^2	τ secs
Dog4 (Aortic occlusion)	10.8	210	2.63
Dog5 (Occlusion of carotid arteries)	9.676	322	3.125

During aortic occlusions there are changes in flow and pressure patterns (Fig 26a). The most striking change occured in the systolic part of the pressure tracing which became biphasic [33]. The peripheral resistance during the occlusions is increased compared with the control situations.

The flow and pressure patterns in dog5, ie. with occlusion of both carotid arteries is shown in Fig (26b).

4.4 Results

4.4.1 IRF calculation by Transform method

The input impedance of dog4 is shown in Fig (27). The modulus seems to have a minimum. The maxima and minima can be seen in Fig (27). The impulse response

function, computed by inverse Fourier transforming the input impedance, after filtering with Dolph-Chebyshev filter is shown in Fig (28a). From the IRF plot, the total arterial compliance was estimated by extrapolating the exponential decay to time zero.

The input impedance for the dog5 (ie. occlusion of both carotid arteries) is in Fig (29). The modulus is found to decrease less rapidly with frequency but, a minimum, as in the case of aortic occlusions is not easily distingiushed. The phase at low frequencies is slightly more negative when both carotids are occluded, but the phase first increases monotonically and then assumes a constant value, as in the control situation. The impulse response function is computed from the input impedance by inverse Fourier transformation. The input impedance is transformed first, without filtering and then with filtering. The plots are shown in Fig (28b).

4.4.2 IRF calculations by Direct methods

Conventional method

The impulse response function of the arterial system of the dog with occlusion of both carotid arteries was computed by the Conventional method. The start times of deconvolution were varied from 0.18 - 0.20 secs. But this method was not successful in recovering the IRF from the input and output time data. This is illustrated in Fig (30a) & (30b).

Gauss-Seidal method

The Gauss-seidal method was then applied to the flow and pressure data from dog5 also did not generate meaningful IRF. This is illustrated in Fig (31b).

Over-relaxation method

The relaxation parameter was varied between 1.1 & 1.5. Different start times were chosen but it resulted in highly distorted IRF's for dog5. This is shown in Fig (32).

Under-relaxation method

As in previous applications, the data were evaluated by considering the relaxation parameter to be 0.01, thus reducing to an Under-relaxation method. This method was applied to the was applied to the flow and pressure data from dog5 (ie. the dog with occluded carotid arteries). The relaxation parameter was set to be 0.01 as seen in Fig (33a). The start times was initially set to be 0.21 secs. Start times prior to 0.21 secs gave very high estimates of compliance from the IRF plot. Start time of deconvolution = 0.215 secs (equal to a start point of 43 samples) resulted in a IRF plot which resulted in a good estimate of compliance which closely agreed with the total arterial compliance computed from the diastolic pressure waveform.

α was then made to be 0.02 and deconvolution was applied to compute the IRF of the arterial system of dog5. This is illustrated in Fig (33b). Start time of deconvolution of t = 0.195 secs yielded a meaningful IRF plot. The estimated compliance from the plot was found to be 338 ($\times 10^{-6}$) $gm^{-1}.cm^4.sec^2$. The total arterial compliance for dog5 as determined from the diastolic pressure waveform was 322 ($\times 10^{-6}$) $gm^{-1}.cm^4.sec^2$.

The results are tabulated as follows:

Table 4.4 Under-relaxation method

Dog	Alpha	Start time secs	Compliance ($\times 10^{-6}$) $gm^{-1}.cm^4.sec^2$	Compliance estimated from exponential fit method
Dog5	0.01	0.21	516	322
		0.215	326	
	0.02	0.18	533	
		0.19	397	
		0.195	338	

The relaxation parameter was varied from 0.03 - 0.09 but it resulted in highly distorted and meaningless impulse response functions for both the dogs.

It was observed once again that there exists a relationship between alpha and the start time as seen in the other 3 dogs. As α was increased, the optimum start times of deconvolution yeilding good estimates of compliance were found to decrease as can be seen in Fig (34).

4.4.3 Reflection Calculations

Reflection calculations can be made from the input impedance though the impulse response function shows reflections quite clearly [6]. Location and amount of reflection can be obtained from the input impedance as follows [26] : at the lowest frequency where the modulus of the impedance is minimal, one-quarter of the wave-length is equal to the length of the system [18]. From the pulse wave velocity and this first minimum,

$$l = c/f_{min} \tag{4.1}$$

where l is the effective length, c is the phase velocity and f_{min} is the lowest frequency where the modulus is a minimum or the phase crosses zero [35]. Similar relations hold for the other minima and maxima of the modulus of the impedance and also for the phase crossings.

Reflection studies can be made from the impulse response function [6]. The impulse response function consists of a series of equidistant peaks. The time interval(ΔT) between peaks is related to the effective length l by

$$l = \Delta T^{*} c/2 \tag{4.2}$$

Reflection studies were conducted for the dogs under occlusion conditions and the reflection computations made from the input impedance and the impulse response function were in agreement.

Chapter 5

Discussion of results

This thesis deals with characterization of arterial system in time domain by applying deconvolution techniques to measured pressure and flow data. Various mathematical methods were investigated to compute the impulse response function directly by deconvolving the the input and output time histories. The data utilized for evaluating the deconvolution techniques consisted of aortic flow and pressure signals derived from (1) a 3-element Windkessel model of the arterial system, (2) a control dog (3) a dog with occlusion of the aorta and (4) a dog during occlusion of both carotid arteries.

The computed impulse response function of the Windkessel model and of the arterial system of the dogs are compared with the appropriate information derived from the input impedance of the arterial system. The input impedance and the impulse response function are equivalent representations but some features of the system are emphasized more clearly by one description than by the other. The input impedance is a frequency domain characterization and characterizes the peripheral resistance and characteristic impedance of the aorta. The Impulse response function is the time domain characterization, emphasizes total arterial compliance and shows reflections more clearly. Hence, the two parameters of interest in this study of the arterial system in time domain are the arterial compliance and wave reflections.

The various mathematical methods investigated in computing the IRF are
(1) Conventional method - by direct numerical evaluation of the convolution integral.
(2) Numerical approximation methods - by using iterative procedures including the relaxation methods.

The parameters that were found to critically influence the successful application of these methods are the start time of deconvolution, the sample rate and in the case of the iterative methods, a relaxation parameter α.

5.1 Windkessel model

The data of a 3-element Windkessel model provide the basis for testing the mathematical methods. The deconvolution procedures applied to the input and output time histories of the Windkessel model yielded results in conformation with the analytical components described by eq. 1.3.

The analytical impulse response function clearly contains a negative exponential function as given by the equation. The compliance value could be estimated from the impulse response function plot by extrapolating the exponential decay to time zero. The results of the IRF using the transform method illustrated in Fig (4) reveal these components. The computed value of the total arterial compliance agree with the model paramter of the Windkessel.

Although the transform method is effective in computing the IRF, the method requires the impedance function to be subjected to a frequency domain filter in order

to eliminate the truncation effects. The Dolph-Chebyshev function [6] used in this method is shown to be an appropriate function. However, it is important to understand that while the smoothing function is effective in control situations, it may pose problems in extracting the IRF in the presence of any reflection phenomena. It is therefore more desirable to develop methods for direct evaluation of the IRF by deconvolving the pressure and flow signals.

In an effort to obtain the impulse response function by direct deconvolution, the Windkessel model data were subjected to direct numerical evaluation procedures. The results are presented in Fig (5a). The application of the deconvolution procedure is severely hampered by the negligibly small flow values. Division by a small flow value will give rise to large errors in the impulse response function. So, the start times of deconvolution procedures were varied, an example of which is shown when t was set to 0.4 secs. The method, however, did not yield meaningful IRF.

In the next set of procedures, various numerical approximation methods were used. Of particular interest are the relaxation methods, in which a relaxation parameter α was introduced to control the stability of the iterative solution of the deconvolution algorithm. Proper choice of α is the key to successful application of this method. If $\alpha < 1$, the system is considered under-relaxed and if $\alpha > 1$, the system is said to be over-relaxed. If $\alpha = 1$, it reduces to the Gauss-Seidal method.

The Over-relaxation method was applied to the data from the Windkessel model. It was found that the method is very sensitive to the noise present in the data It was not possible to derive meaningful impulse response functions using this method. In spite of varying the value of the relaxation parameter and the start times for de-

convolution, the impulse response function showed spurious oscillations.

When the relaxation parameter was set equal to 1.0, reducing to the Gauss-Seidal method, the derived impulse response function did not follow an exponential decay as can be seen in Fig (5c) & Fig (5d). Varying the start times did not seem to be effective in producing the desired IRF.

The Under-relaxation method was next considered with the relaxation parameter α varied between 0.01 and 0.05. Various start points were chosen, examples of which are given in Fig (7). At t = 0.4 secs corresponding to a point in the rising segment of the systolic pressure waveform, the flow values were at the peak. Earlier start times with very small flow values (nearly zero) resulted in incongruous impulse response functions. The compliance value was estimated from the IRF plot by extrapolating the exponential part to time zero.

When $\alpha = 0.04$ and when deconvolution was initiated at 0.52 secs, the IRF plot yeilded a value of compliance which closely approximated the model parameter.

Various values of the relaxation parameter were investigated to obtain better estimates of the compliance. α was varied from 0.05 to 0.09 resulting in reliable plots with good estimates of compliance. This is indicated in Fig (8) and in table (3.1). It can be observed in Fig (8) that for $\alpha = 0.05$, as the start times were increased from 0.50 secs to 0.52 secs, the impulse response function gave lower estimates of compliance. This is given in Table 3.1. If the start time was increased above 0.55 secs, it resulted in a very low estimate of compliance. Similarly, decreasing the start time to approximately 0.45 secs resulted in very high estimates of compliance in the range

of 1000 ($\times 10^{-6}$) gm^{-1}. $cm^4.sec^2$. This observation held true for α between 0.06 & 0.09.

The start time of deconvolution proved to be a very important factor in the accurate estimation of the compliance. It was observed that as the value of the relaxation parameter was increased, the times at which deconvolution was initiated to yield a good value of compliance, were found to decrease. This is illustrated in Fig (14a). It is obvious the influence of start time is critical in the relaxation procedure.

The input and output data from the Windkessel model were sampled at 256 samples/sec. Then, the Under-relaxation method was investigated. The earlier analysis was done at 100 samples/sec.

The Under-relaxation method proved to be effective in extracting the impulse response function. When α was set equal to 0.01, the IRF exhibited an initial peak followed by an exponential decay as expected. The value of the compliance estimated from the plot closely matched the model parameter C = 60 ($\times 10^{-6}$) $gm^{-1}.cm^4.sec^2$ when the deconvolution procedure was activated at t = 0.55 secs which corresponded to a start point of 141 samples.

Values of α between 0.02 to 0.09 gave good IRF plots with good estimates of compliance. This is tabulated in Table 3.3. As before, as the value of the relaxation parameter was increased, the optimum start times yielding reasonable estimates of compliance was found to decrease. This is illustrated in Fig (14b). There seems to be a nearly linear relationship between α and the start time as seen before with the sample rate of 100 samples/sec.

Also, for a particular value of α, when the start times of deconvolution were increased, the compliance values computed from the IRF plots decreased as could be observed in Table 3.3.

5.2 Dogs under control conditions

The heart rates for the dog under control conditions was set equal to 32 beats/min. 85 beats/min & 129 beats/min with the data sampled at 200 samples/sec with the three cases labelled as doghr1, doghr2 & doghr3.

The input impedance of the arterial system of the dog computed by Fourier transforming the flow and pressure data measured in the dog is illustrated in Fig (16). The corresponding impulse response functions calculated by the transform method can be seen in Fig (17). Total arterial compliance found by an extrapolation of the exponential decay to zero time (after correction of the periodic excitation T) was found to match closely with the compliance calculated from the diastolic pressure decay.

Then the various deconvolution methods were applied to the pressure and flow data from the dog under different heart rates. The Conventional method, Gauss-Seidal method & Over-relaxation method were found to be very sensitive to the noise in the flow and pressure data and it was not possible to derive meaningful impulse response functions as is evident in Fig (18), Fig (19), Fig (20) & Fig (21). The results did not improve for varying the start times of deconvolution.

Only the Under-relaxation method seemed to be the most effective in extracting the impulse response function. Values of α equal to 0.01, 0.02 & 0.03 resulted in impulse response functions which has an initial peak, gradually following the expected

negative exponential curve. This is illustrated in Fig (22), Fig (23) & Fig (24). The start times were varied and the impulse response functions were computed. It was seen that with values of α ranging from 0.01 to 0.03 and with start times between 0.3 secs to 0.32 secs, the IRF computed by the Under-relaxation method gave good estimates of compliance in accordance with the value estimated from the diastolic pressure decay.

For doghr3, values of α between 0.01 and 0.03 and with start times of deconvolution between 0.24 secs and 0.28 secs, the IRF plot gave reliable estimates of compliance.

When deconvolution was initiated between 0.3 secs & 0.32 secs and with α between 0.01 to 0.03, the IRF of the arterial system of doghr1 computed by the Under-relaxation method gave accurate estimates of compliance.

It was observed that these start times correspond to a time segment in the pressure waveform just after the systolic peak pressure is reached - Fig (15). For all the three cases considered, with the relaxation parameter between 0.01 to 0.03 and with start times which coincide with that part of pressure wave just after the peak, the computed IRF gave good estimates of compliance.

The Under-relaxation method was not effective in extracting the impulse response function from the flow and pressure data when the relaxation parameter α was increased above 0.03 for all the three subjects. It resulted in distorted impulse response functions.

Another interesting observation was that similar to the Windkessel model, as the values of the relaxation parameter was ioncreased, the times at which deconvolution is initiated was found to decrease. This is illustrated in Fig (25).

Although the impulse response function of the dogs follow the Windkessel pattern, some oscillations are noticable and they suggest the presence of reflection sites in the system. From the knowledge of the phase velocity of the control dog [6] [33] and the location of the first peak in the impulse response function (computed with $\alpha = 0.01$ and start time = 0.32 secs), the location of the reflection point closest to the heart is calculated to be 13 cms. (See eq. 4.2).

Since the impulse response function and the input impedance contain the same information, the location of the reflection point closest to the heart was calculated from the input impedance of the arterial system of doghr2. A minimum in the modulus of the impedance was noted at 6 Hz and using eq. 4.1, the location of the reflection site was calculated to be 17 cms.

The reflection site calculated from the input impedance and the impulse response function of the arterial system of doghr1 & doghr3 were found to match.

5.3 Dogs under occlusion conditions

Two dogs were considered :-

(1) Dog with aortic occlusion - Dog4.

(2) Dog with occlusion of both carotid arteries - Dog5.

The heart rate for dog4 is 137 beats/min and that for dog5 is 151 beats/min. First

the impulse response function of the arterial system of dog4 & dog5 were computed by the transform method by inverse Fourier transforming the input impedance of dog4 & dog5 as illustrated in Fig (27). The compliance estimated from the IRF plots coincided with the compliance values calculated from the diastolic pressure decay.

Then the various deconvolution procedures were investigated to compute the impulse response function from the measured pressure and flow data of dog5. The Conventional, Gauss-Seidal and the Over-relaxation method resulted in highly distorted and meaningless impulse response functions due to noise effects.

The Under-relaxation method was then applied to the flow and pressure data from dog5. When α was equal to 0.01 & 0.02, with start times of deconvolution in the range 0.195 secs - 0.215 secs, this method gave rise to meaningful IRF plots. The compliance values calculated from the plots matched with the compliance value estimated from the diastolic pressure decay. But values of α greater than 0.02 did not give rise to the expected impulse response function with an exponential decay.

Reflection calculations were recorded for dog5. Reflection computations in time domain (ie. from the Impulse Response Function) and in frequency domain (ie. Input Impedance) were compared and found to coincide. Reflections were seen much better in the impulse response function.

Bibliography

[1] Bergel, D.H. - "The Dynamic elastic properties of the arterial wall".

[2] O'Rourke, M.F. Taylor, M.G., "Input Impedance of the systemic circulation", Circ. Res., vol. 20, pp. 365 - 380, 1967.

[3] Sipkema, P., Westerhof, N. Randall, O.S., "The arterial system characterized in the time domain", Cardiovasc. Res., vol. 14, pp. 270 - 279, 1980.

[4] Burkhoff, "Assessment of Windkessel as a model of aortic input impedance", Am. J. of Physiol., 1988.

[5] Bergel, D.H. Milnor, W.R., "Pulmonary vascular impedance in the dog", Circ. Res., vol. 16, pp. 410 - 415, 1965.

[6] S.Laxminarayan, Sipkema, P. Westerhof, N., "Characterization of the arterial system in time domain", IEEE trans. in Biomed. Eng., vol. BME-25, pp. 177 - 183, 1978.

[7] Latson, T.W. Hunter, W.C., "Time sequential prediction of ventricular-vascular interactions", Am. J. of Physiol., vol. 251, pp. H1341 - H1353, 1986.

[8] Laxminarayan, R., "Deconvolution techniques", Masters thesis, NJIT, 1986.

[9] M.E.Valentinuzzi, E.M.Volache - "Discrete Deconvolution".

[10] Segre, G - "Compartmental models in the analysis of intestinal absorption".

[11] A.M.Cohen - "Numerical Analysis".

[12] M.K.Jain, S.R.K.Iyengar - "Numerical methods for Scientific and Engineering computations".

[13] N.Westerhof, G.Elzinga G.C.Van den Bos, " Influence of central and peripheral changes on the hydraulic input impedance of the systemic arterial tree", Med. Biol. Eng., vol. 11, pp. 710 - 723, 1973.

[14] Stephanie M.Toy, J.Melbin Noordergraf, A. "Reduced models of the arterial tree", IEEE Trans. Biomed. Eng., vol. BME-32, 1985.

[15] A.C.Simon, M.E.Safar, J.A.Levenson, G.M.London, B.I.Levy N.P.Chau "An evaluation of large arteries compliance in man",

[16] Zharong Liu, Kenneth P.Brin Frank C.P.Yin, "Estimation of total arterial compliance - an improved method and evaluation of current methods", Am. J. of Physiol., 1986.

[17] S.Laxminarayan, R.Laxminarayan, G.J.Langewouters A.V.D.Vos, "Computing total arterial compliance of the arterial system from its input impedance", Medi. Biol. Eng., vol. 17, pp. 623 - 628, 19

[18] W.Nichols Michael F.O'Rourke, "MacDonald's Blood flow in arteries",

[19] William Hunter Noordergraf, A., " Can impedance characterize the heart? ", J. Appl. Physiol., vol. 40, pp. 250 - 252, 19

[20] N.Westerhof, G.Elzinga P.Sipkema, "An artificial arterial system for pumping hearts",

[21] E.O.Attinger D.A.MacDonald, "Use of fourier series for the analysis of biological systems". Biophys. J., vol. 6, pp. 291 - 304, 1966,

[22] Kenneth B.Campbell, Roberto Burattini, D.L.Bell G.C.Knowlen, "Time domain formulation of assymetric T-tube model of the arterial system", Am. J. of Physiol., 1990.

[23] Piene, H., "Interaction between the right ventricle and its arterial load: a quantitative solution", Am. J. of Physiol., vol.238, pp. H932 - H937, 1980.

[24] Guyton, "Human Physiology".

[25] S.Laxminarayan, R.Laxminarayan. S.Chatterjee, O.Mills, J.Rhonda & E.D.Weitzman, "Linear systems analysis applications in the study of arterial hemodynamics",

[26] N.Westerhof, G.C.Van den Bos, S.Laxminarayan, "Arterial reflections"

[27] P.Sipkema & N.Westerhof, " Time domain reflectometry in a model of the arterial system",

[28] Samuel D.Conte & Carl de Boor, "Elementary Numerical Analysis",

[29] M.T.Jong, " Methods of discrete signals and systems analysis",

[30] R.Milnor, "Hemodynamics",

[31] S.J.Morris, J.P.Woodcock & P.N.T.Wells - "Impulse response of a segment of artery derived from trans-cutaneous blood- velocity measurements".

[32] C.T.Ting, Kenneth P.Brin, S.J.Lin, S.P.Wang, M.S.Chang & Frank C.P.Yin, "Arterial hemodynamics in hypertension", J. Clinical. Inevst., vol. 78, pp. 1462 - 71.

[33] G.C.Van den Bos, N.Westerhof, G.Elzing & P.Sipkema, "Reflection in the systemic arterial system: effects of aortic and carotid occlusion", Cardiovasc. Res., vol. 10, pp. 565 - 573, 1976.

FIG (1)

Windkessel model.

Parameters are : -

Peripheral resistance, R_p = 20 K

Characteristic Imepdance, R_c = 1.2 K

Capacitance, C = 60 μF

FIG (1)

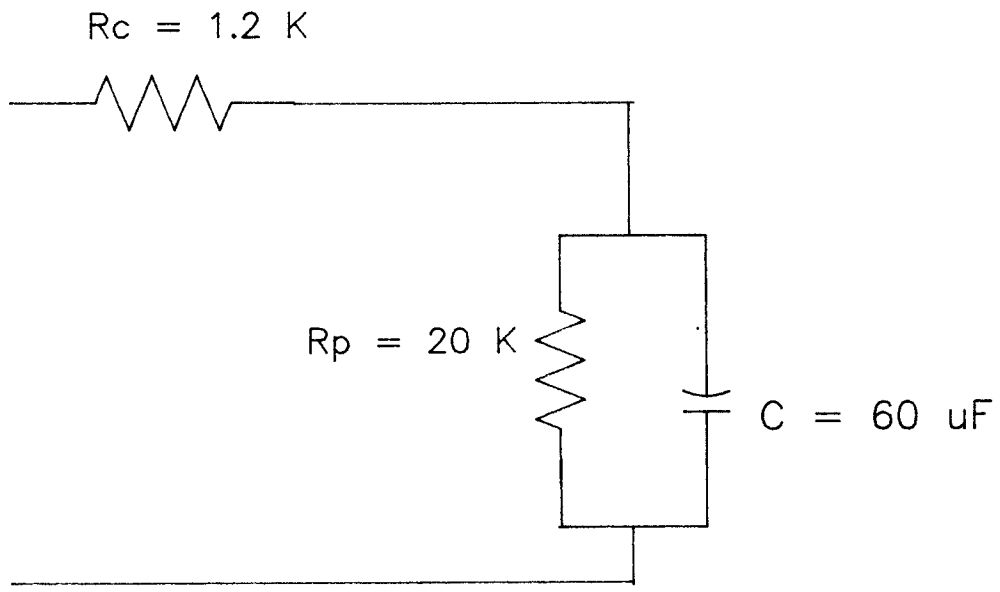

FIG (2)

Flow and pressure waveforms obtained from a 3-element Windkessel model - Fig (1).

Model parameters are as follows:

Peripheral Resistance : $R_p = 20K$,

Characteristic Impedance : $R_c = 1.2K$

Capacitance : $C = 60\mu F$.

FIG (2)

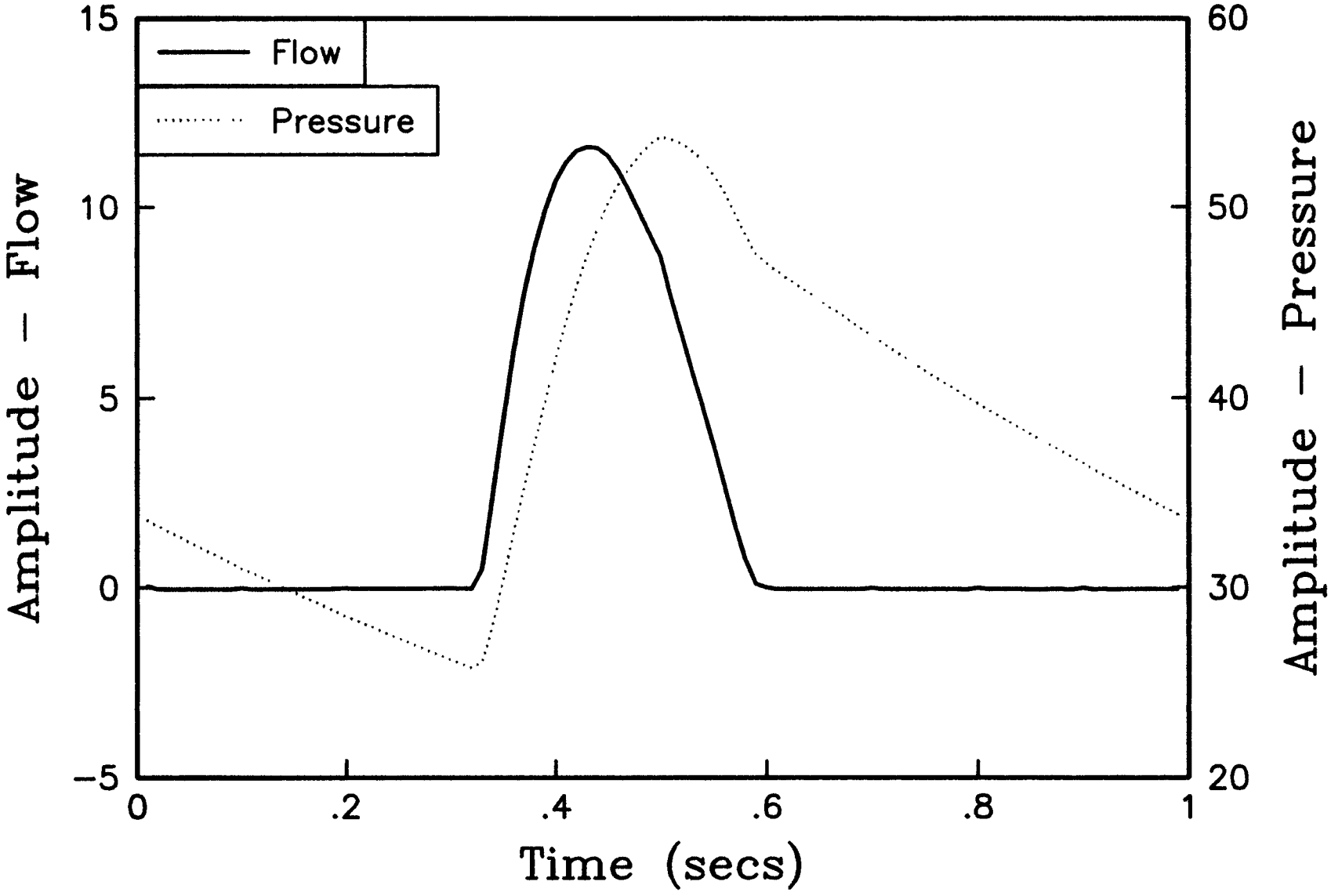
Flow
Pressure
15
10
5
0
−5
60
50
40
30
20
0
.2
.4
.6
.8
1
Amplitude − Flow
Amplitude − Pressure
Time (secs)

FIG (3)

Input Impedance of the 3-element Windkessel model.

(Top : Modulus & bottom : Phase in degrees).

FIG (3)

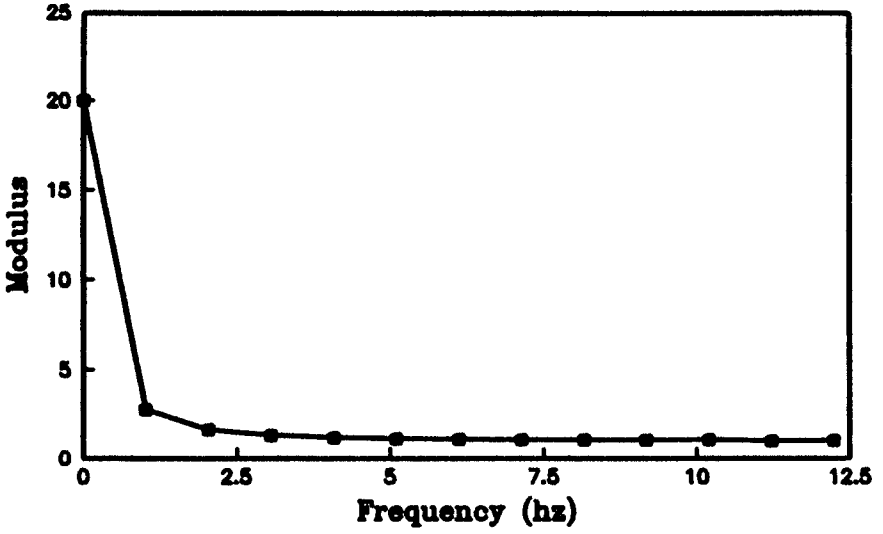
25
20
15
10
5
0
Modulus
0
2.5
5
7.5
10
12.5
Frequency (hz)

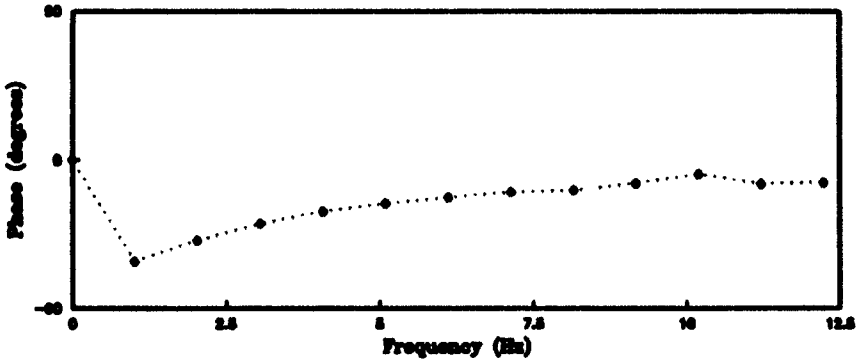
90
0
-90
Phase (degrees)
0
2.5
5
7.5
10
12.5
Frequency (Hz)

FIG (4)

Impulse response function of the Windkessel model obtained from the Input Impedance, without filtering and with filtering before transformation to time domain.

The Dolph-Chebyshev filter was chosen to be the filter.

Filter parameters are as follows :

Ripple factor = 100,

No. of harmonics = 12.

FIG (4)

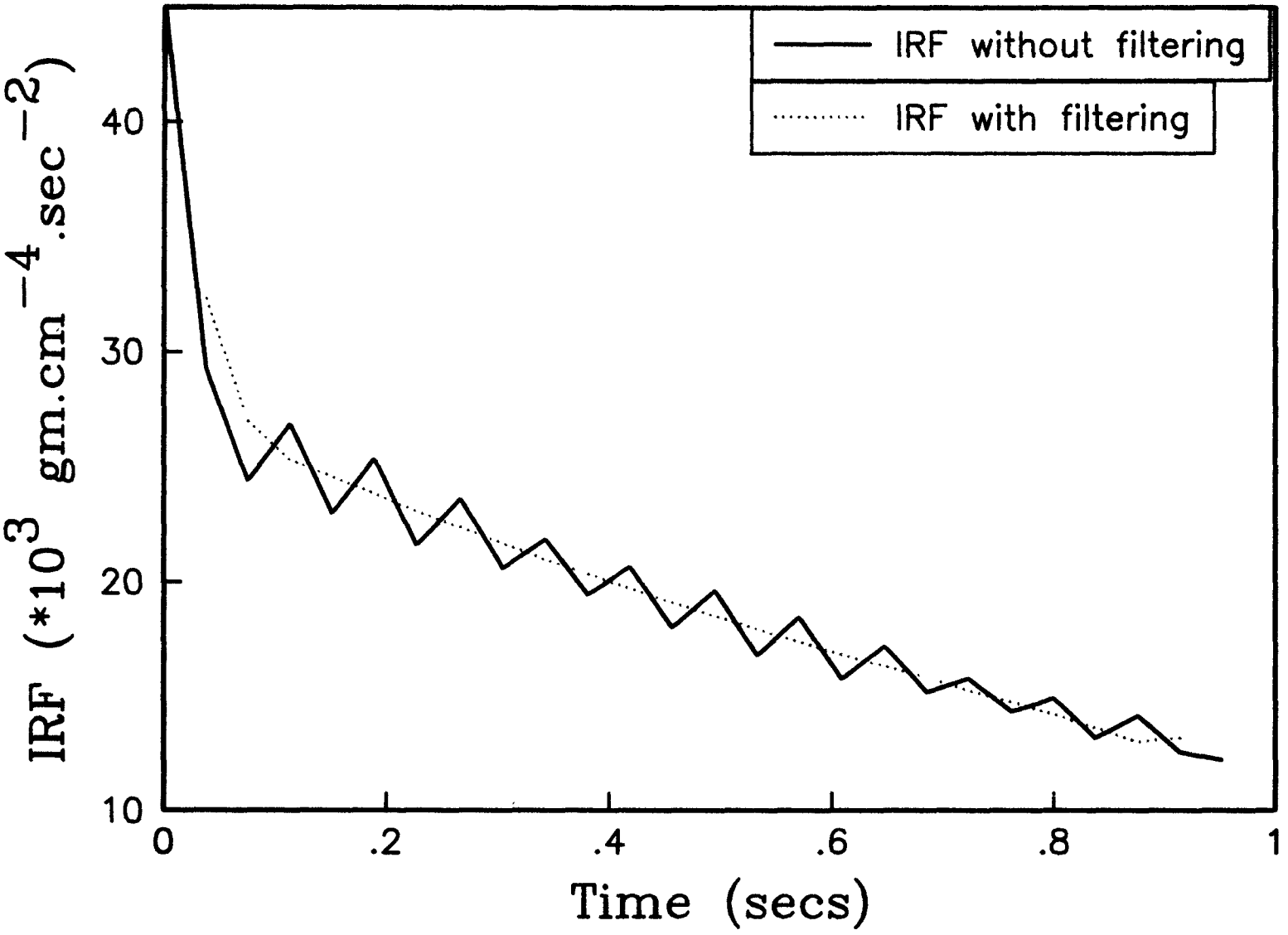
IRF without filtering
IRF with filtering
IRF (*10^3 gm.cm^-4.sec^-2)
40
30
20
10
0
.2
.4
.6
.8
1
Time (secs)

FIG (5)

Fig (5a) & Fig (5b) - Impulse response function of the Windkessel model computed by the Conventional method. Sample rate = 100 samples/sec. A critical aspect of computing the impulse response function is the appropriate choice of the start point.
The following start times were used in computing the IRF.
t = 0.4 secs, 0.45 secs, 0.50 secs & 0.55 secs.

Fig (5c) & Fig (5d) - Impulse response function of the Windkessel model computed by the Gauss-Seidal method. Start times were varied from 0.40 secs to 0.55 secs.

FIG (5a)

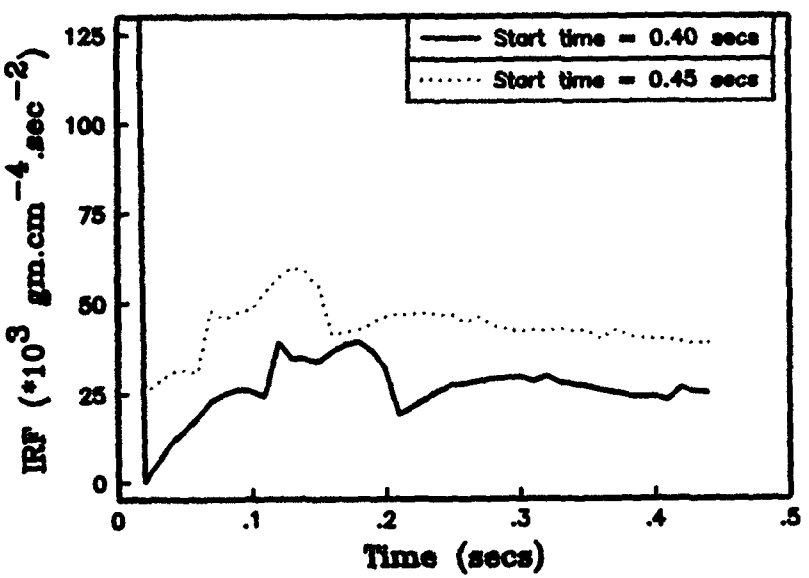

FIG (5b)

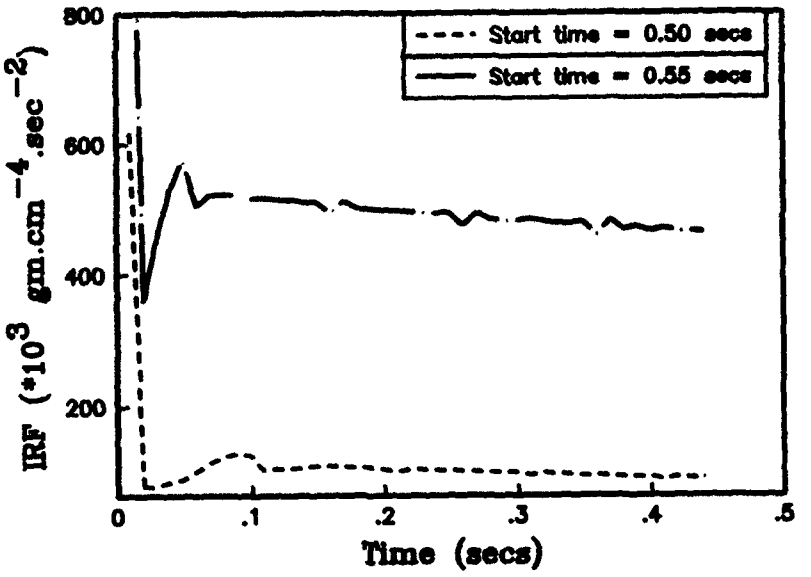

FIG (5c)

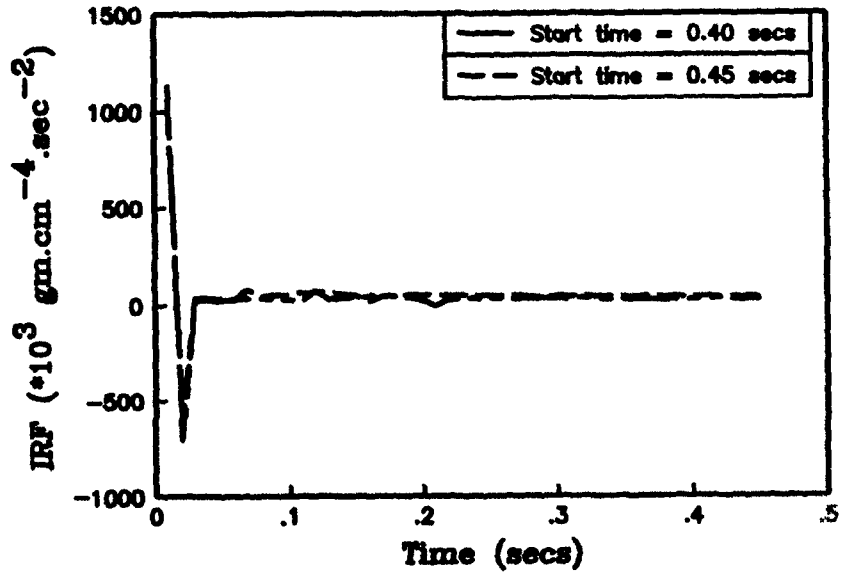

FIG (5d)

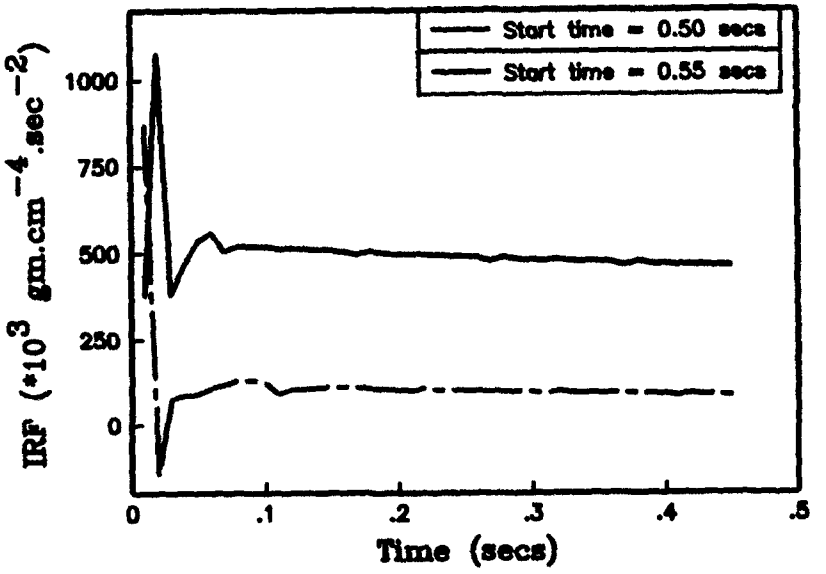

FIG (6)

The Over-Relaxation method was used to calculate the IRF. Alpha was chosen to be = 1.1.

Fig (6a) - IRF when deconvolution was initiated at time t = 0.4 secs and time t = 0.5 secs.

Then the relaxation parameter was taken to be = 1.5.

Fig (6b) - IRF when deconvolution was initiated at time t = 0.4 secs and time t = 0.5 secs.

FIG (6a)

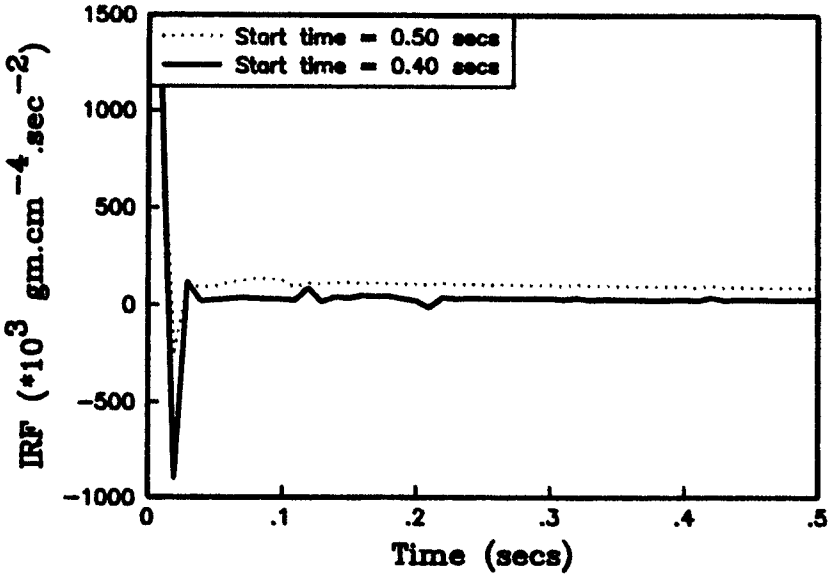
Start time = 0.50 secs
Start time = 0.40 secs
IRF (*10^3 gm.cm^-4.sec^-2)
1500
1000
500
0
-500
-1000
0
.1
.2
.3
.4
.5
Time (secs)

FIG (6b)

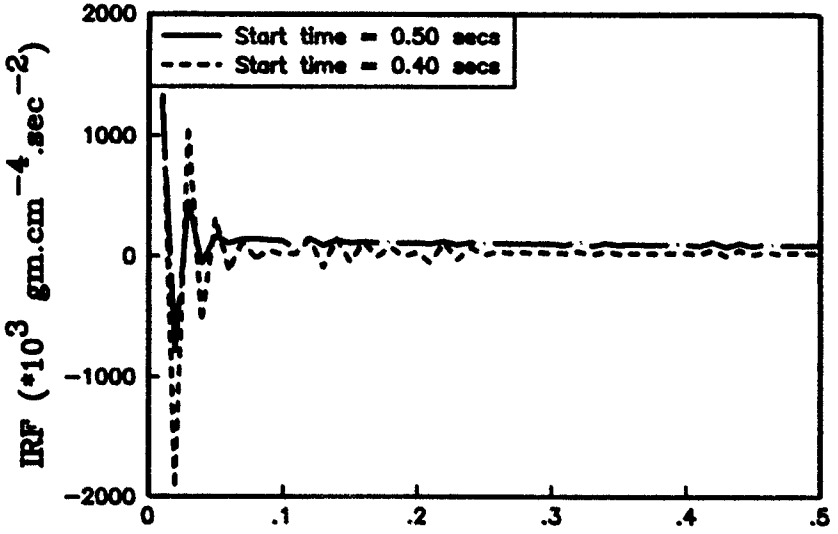
Start time = 0.50 secs
Start time = 0.40 secs
IRF (*10^3 gm.cm^-4.sec^-2)
2000
1000
0
-1000
-2000
0
.1
.2
.3
.4
.5

FIG (7)

Impulse response functions computed using the Under-relaxation method. The relaxation parameter α was varied from 0.01 - 0.04.

$\alpha = 0.01$ - Fig (7a).

$\alpha = 0.02$ - Fig (7b).

$\alpha = 0.04$ - Fig (7c).

$\alpha = 0.05$ - Fig (7d).

Different start times were chosen. The compliance value was estimated from the IRF plots by extrapolating the exponential decay to time zero.

FIG (7a)

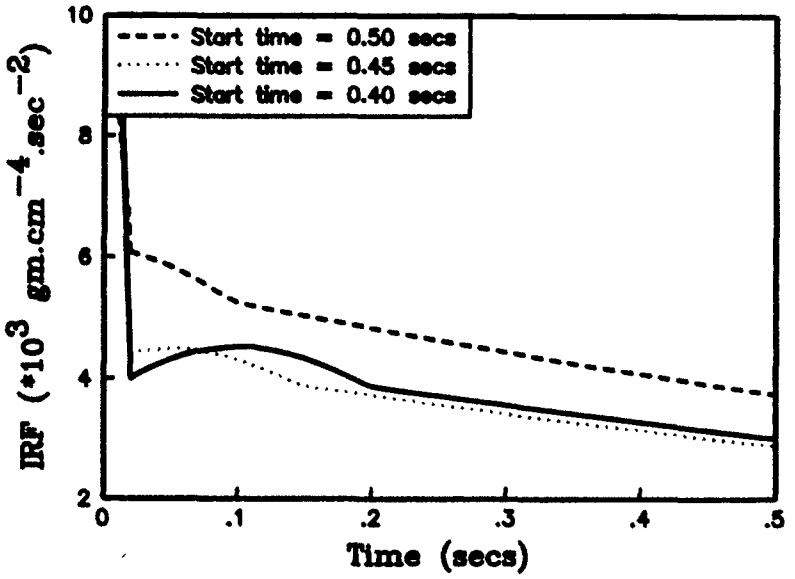

FIG (7b)

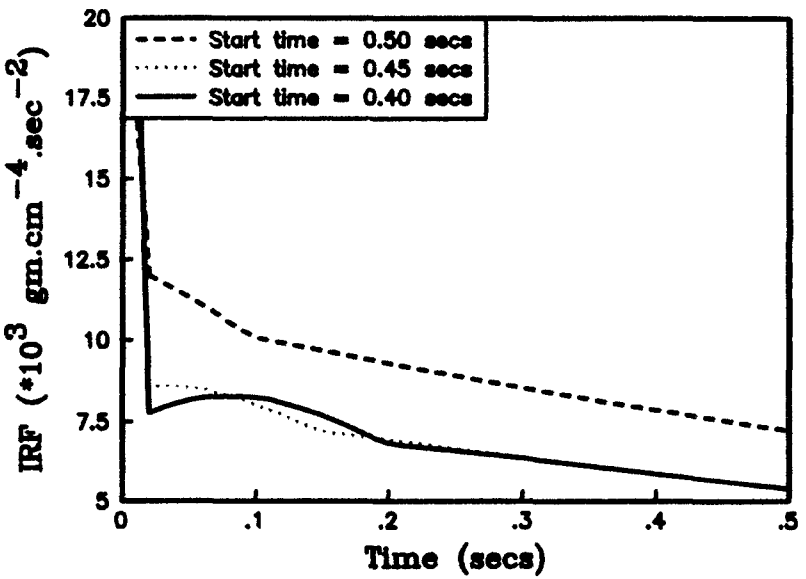

FIG (7c)

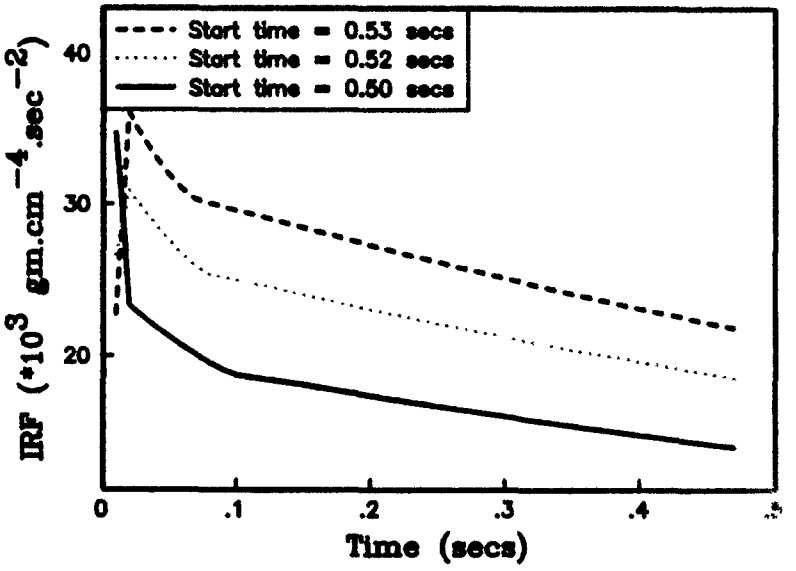

FIG (7d)

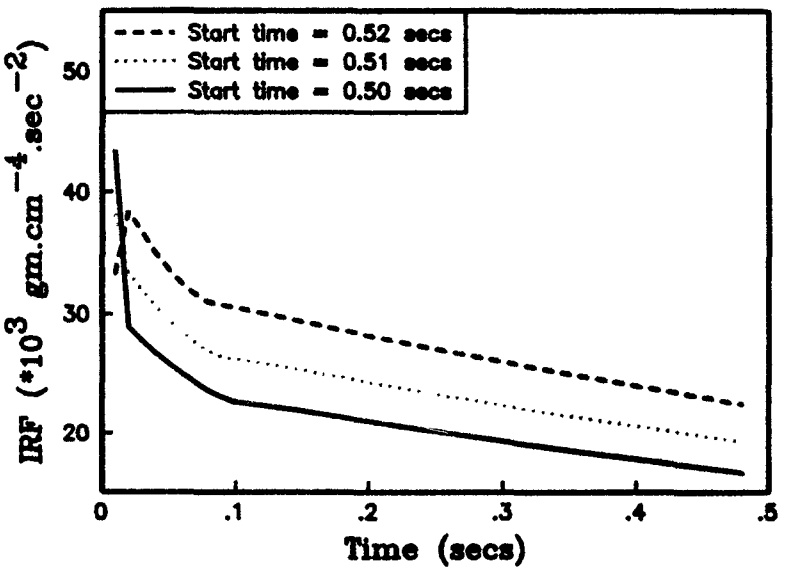

FIG (8)

The relaxation parameter was varied from 0.06 - 0.09 at different start times and the impulse response functions were computed for each case.

$\alpha = 0.06$ - Fig (8a).

$\alpha = 0.07$ - Fig (8b).

$\alpha = 0.08$ - Fig (8c).

$\alpha = 0.09$ - Fig (8d).

FIG (8a)

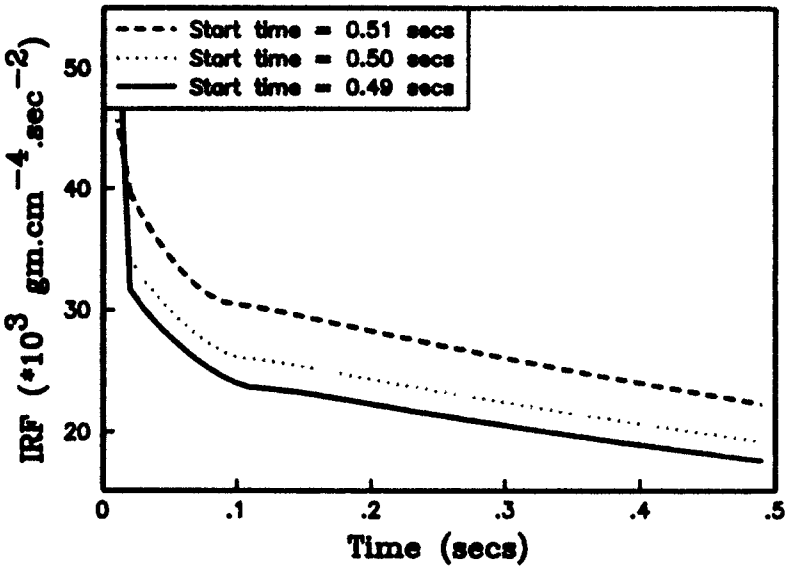

FIG (8b)

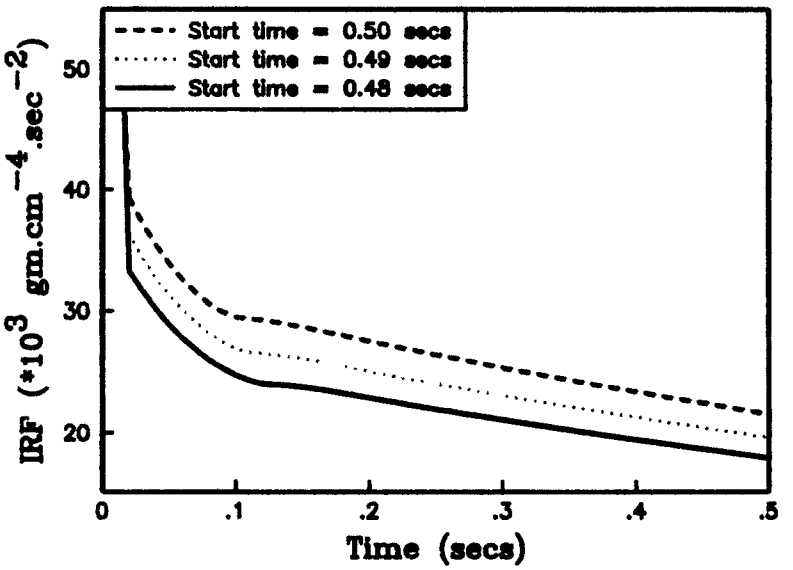

FIG (8c)

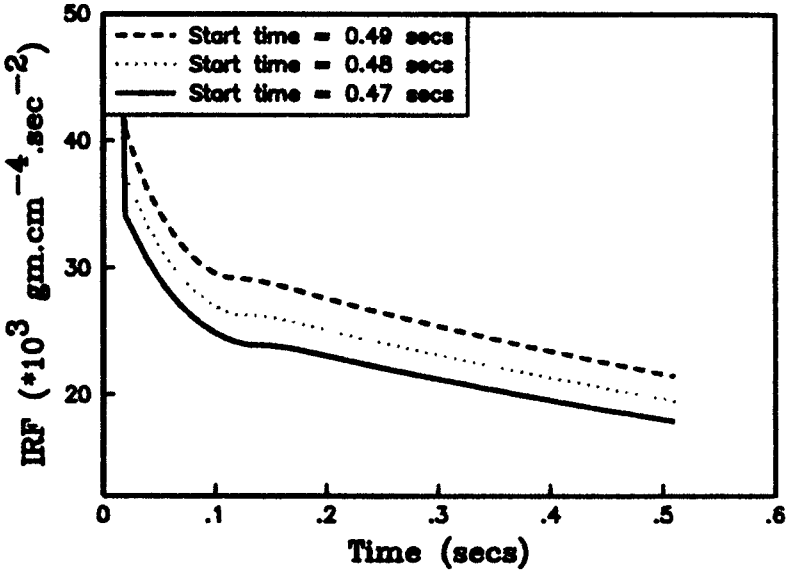

FIG (8d)

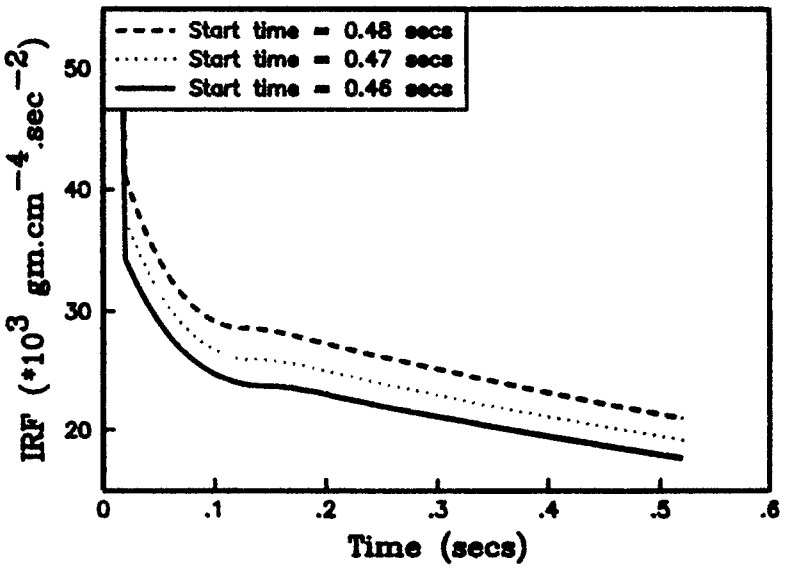

FIG (9)

Fig (9a) & (9b) - Input and output data from the Windkessel model sampled at 256 samples/sec were subjected to the Conventional method. Start times were varied from 0.4 secs - 0.55 secs.

Fig (9c) & (9d) - Impulse response function of the Windkessel model computed by the Gauss-Seidal method at various start times.

FIG (9a)

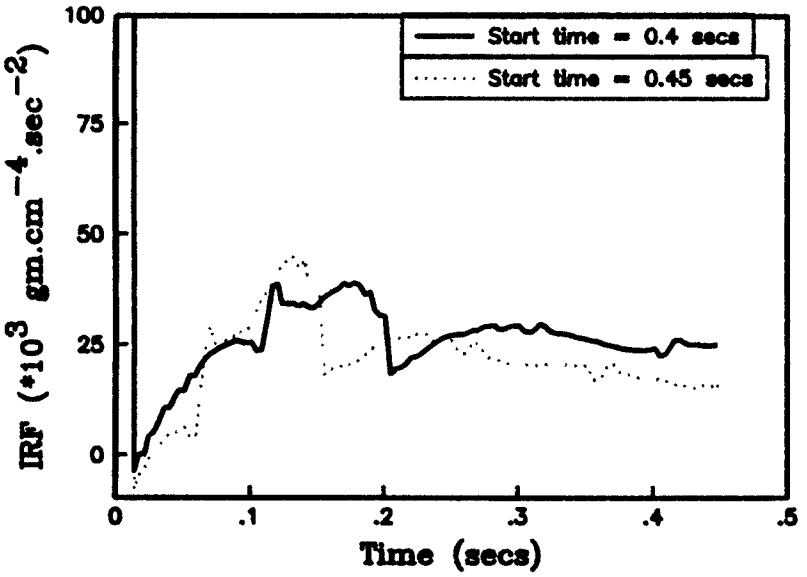

FIG (9b)

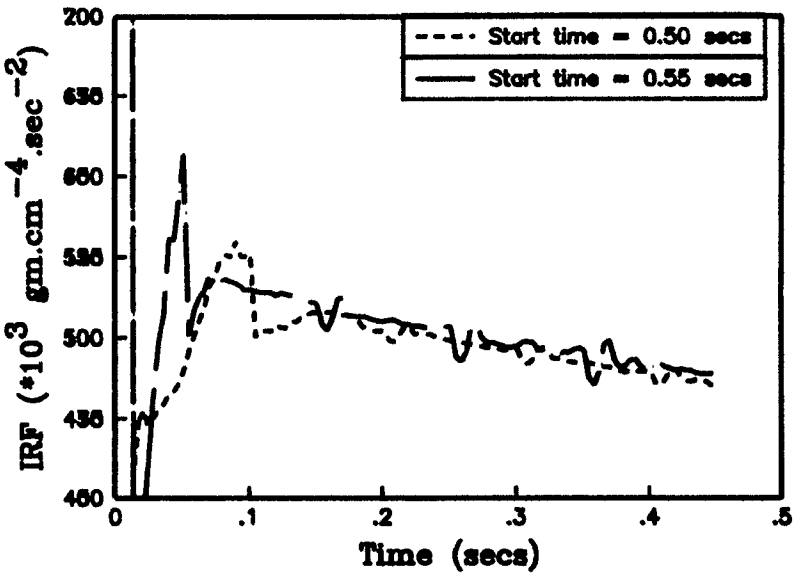

FIG (9c)

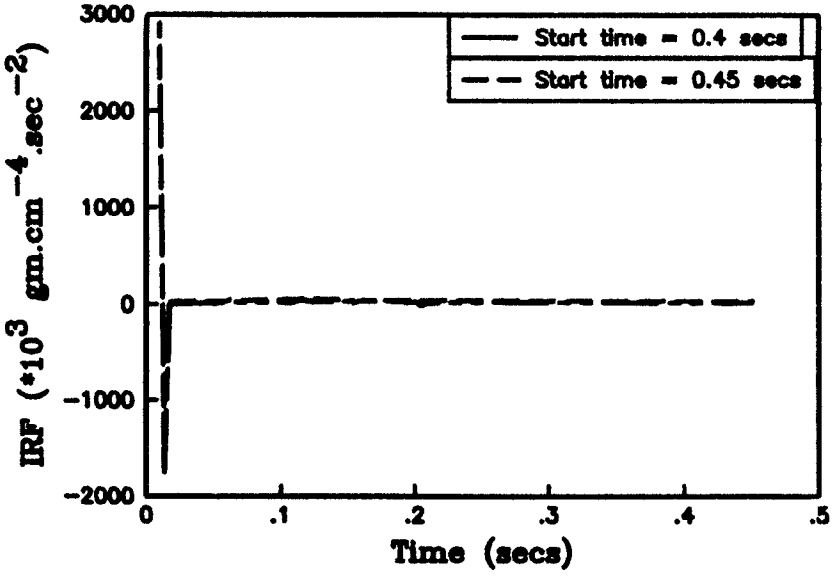

FIG (9d)

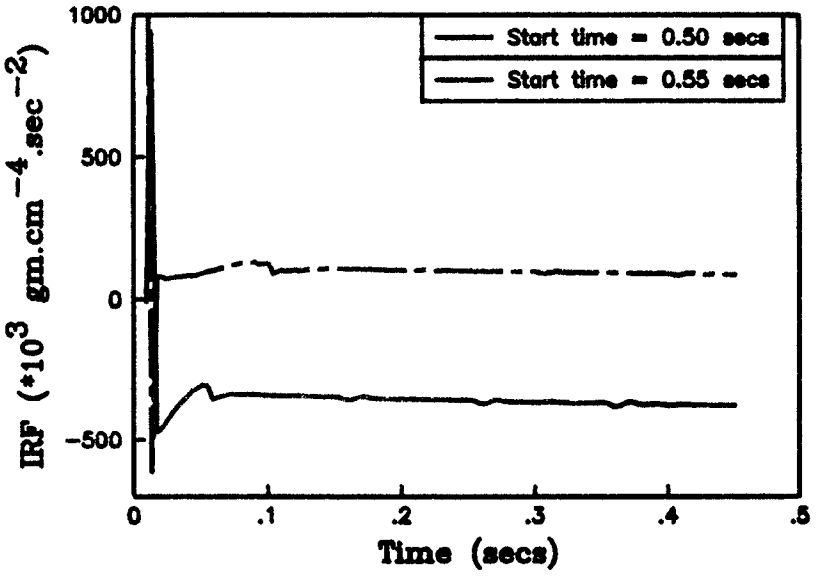

FIG (10)

Over-relaxation method was used to compute the IRF. It gave rise to meaningless impulse response functions.

FIG (10a)

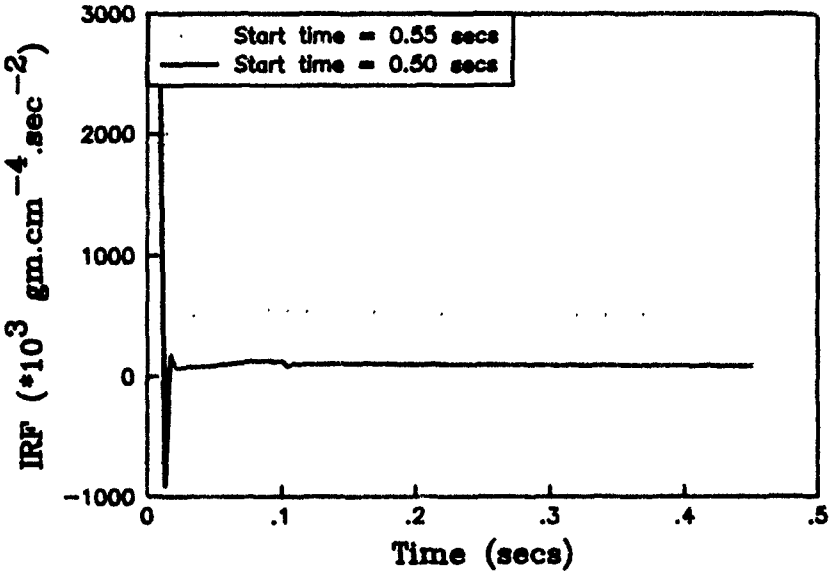

FIG (10b)

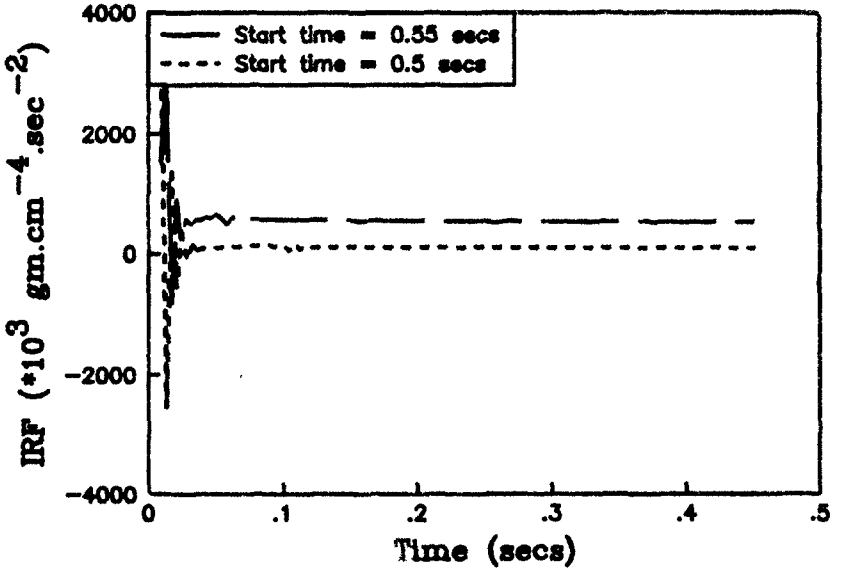

FIG (11)

The Under-relaxation method was used to compute the impulse response function when the input and output time histories from the Windkessel model were sampled at 256 samples/sec.

The relaxation parameter was varied from 0.01 - 0.04 at different start times.

$\alpha = 0.01$ - Fig (11a).

$\alpha = 0.02$ - Fig (11b).

$\alpha = 0.03$ - Fig (11c).

$\alpha = 0.04$ - Fig (11d).

FIG (11a)

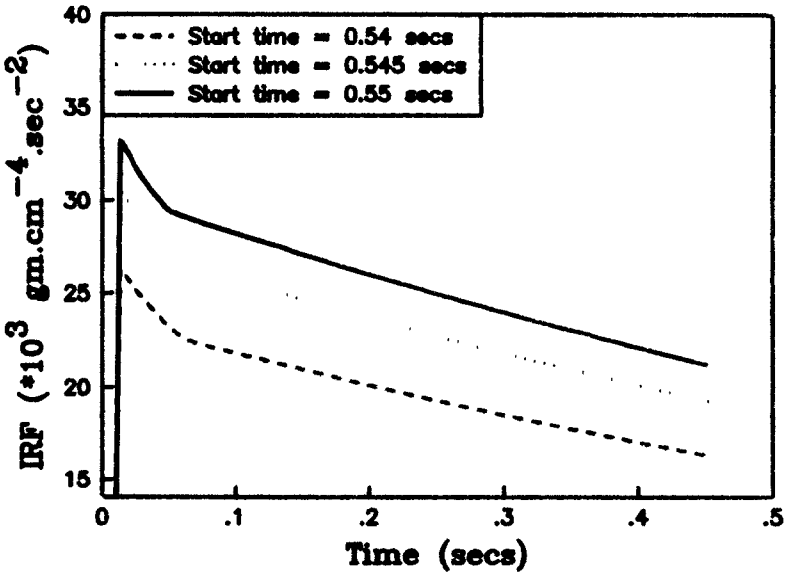

FIG (11b)

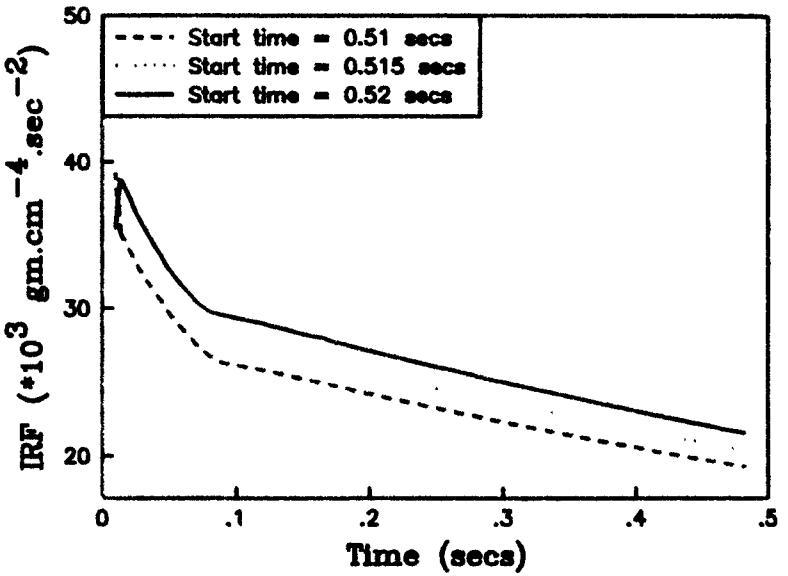

FIG (11c)

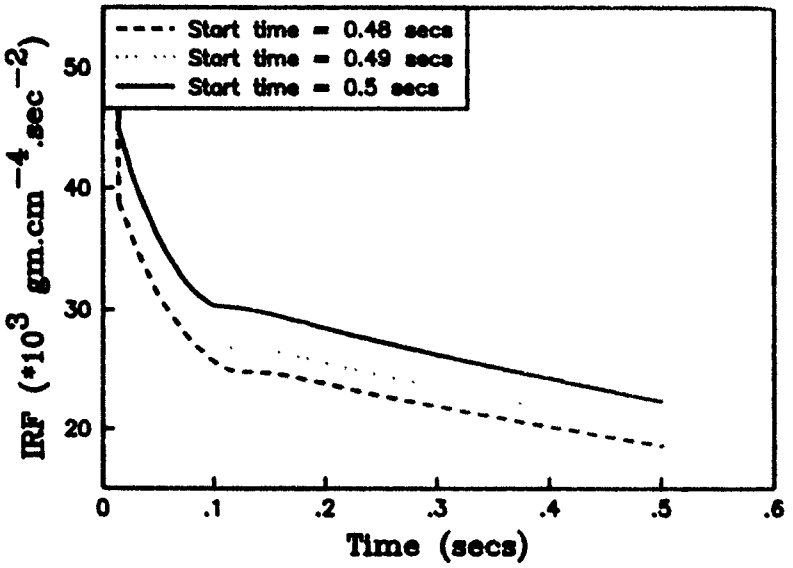

FIG (11d)

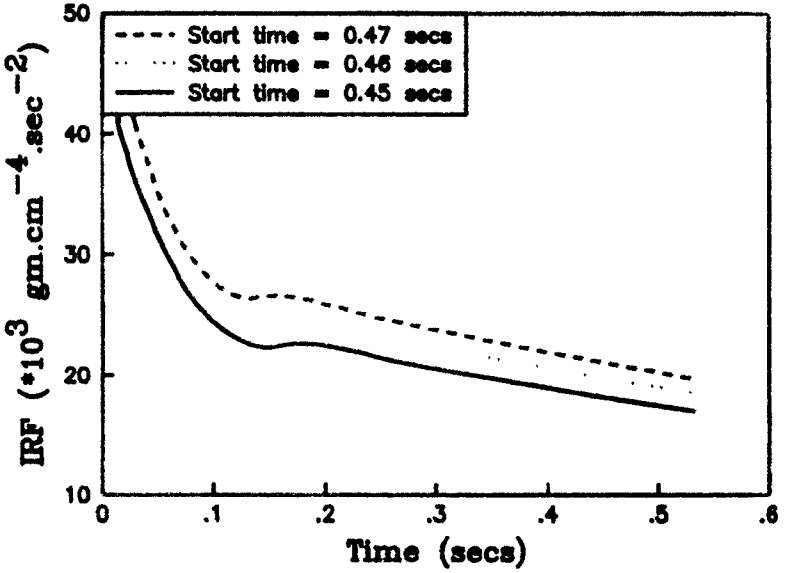

FIG (12)

Deconvolution was performed by the Under-relaxation method with the relaxation parameter α = 0.05, 0.06, 0.07 & 0.08. The corresponding IRF plots are seen in Figs (12a), (12b), (12c) & (12d).

FIG (12a)

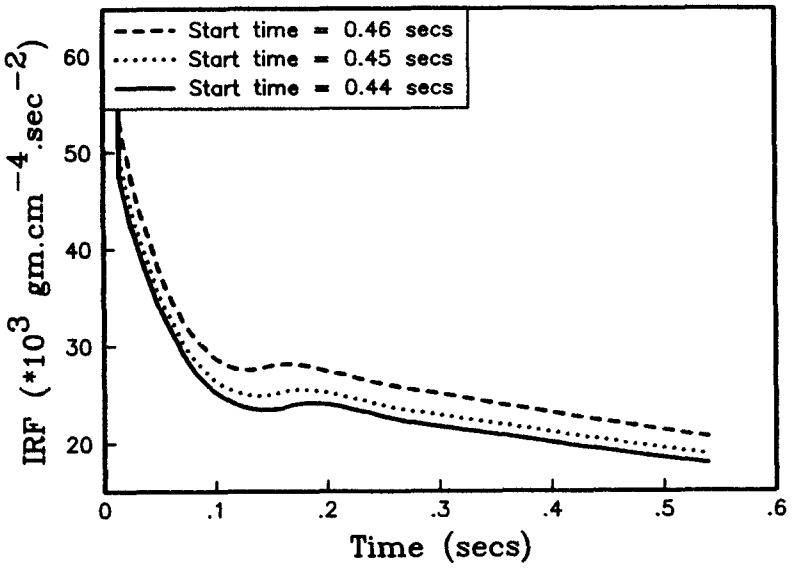

FIG (12b)

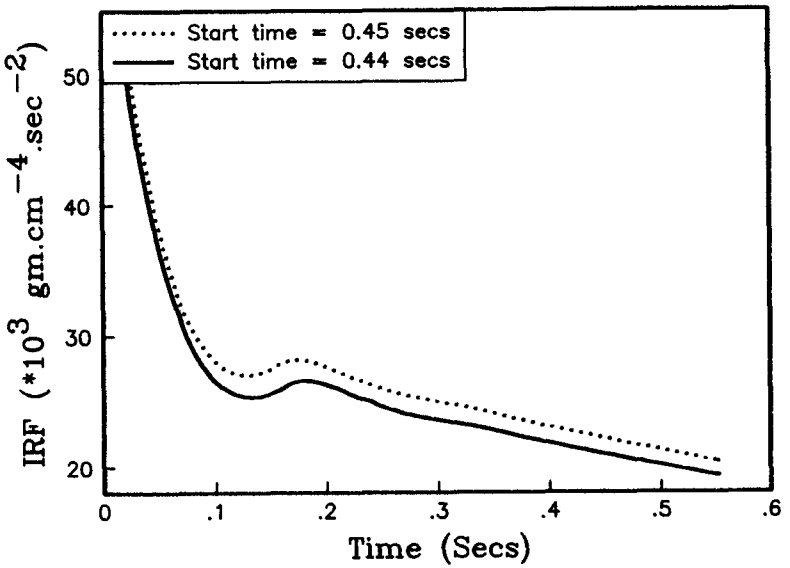

FIG (12c)

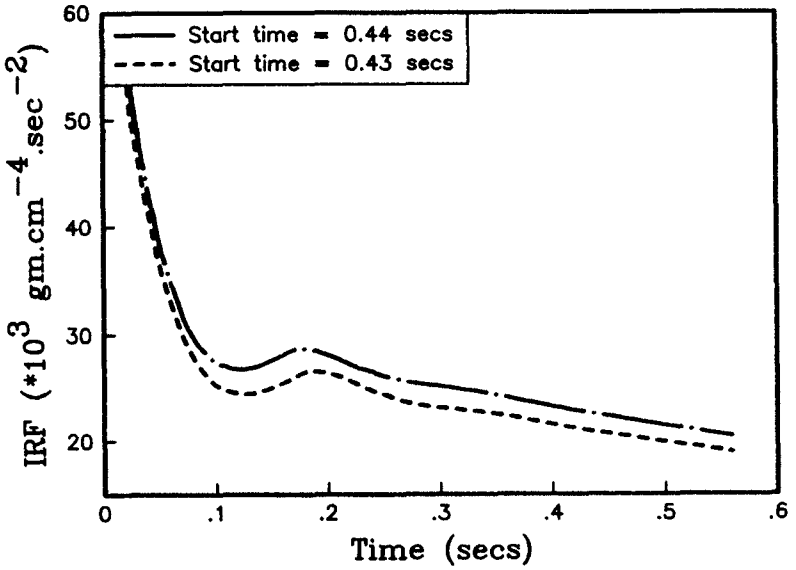

FIG (12d)

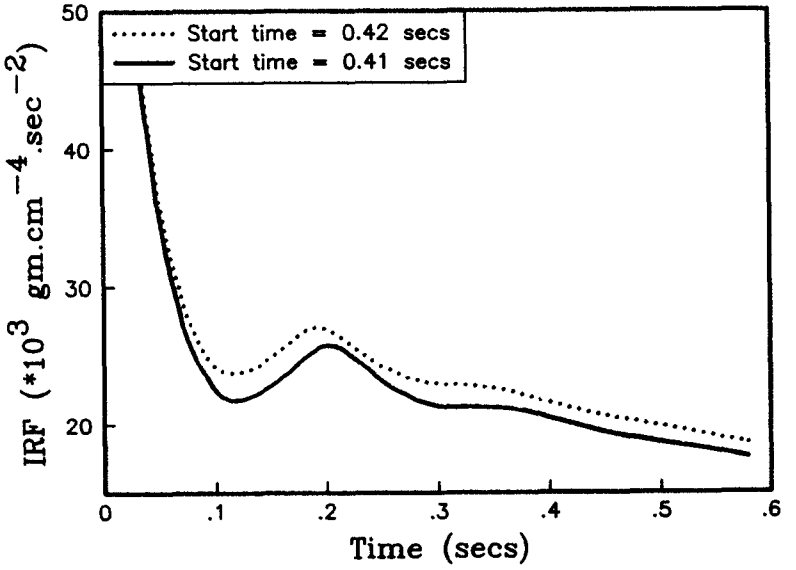

FIG (13)

The relaxation parameter was changed to 0.09 and 0.1 and the impulse response function was computed by the Under-relaxation method. This can be seen in Fig (13a) & (13b) respectively.

FIG (13a)

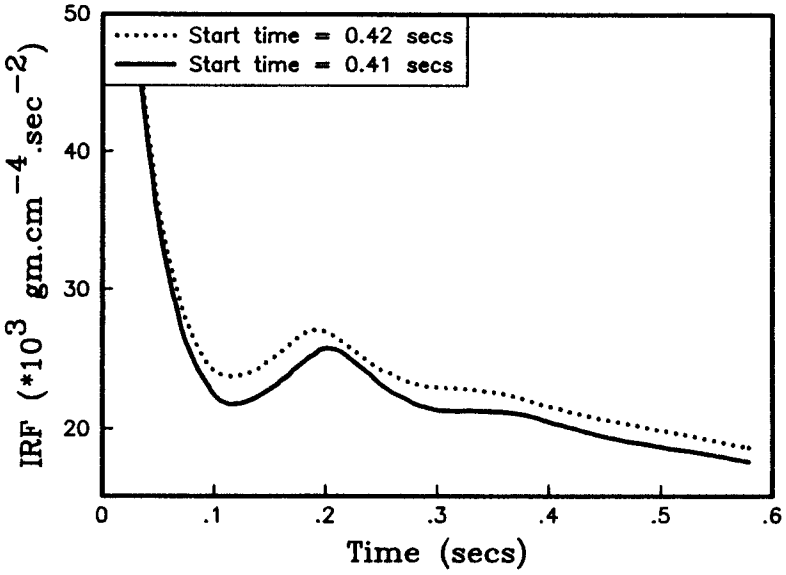

FIG (13b)

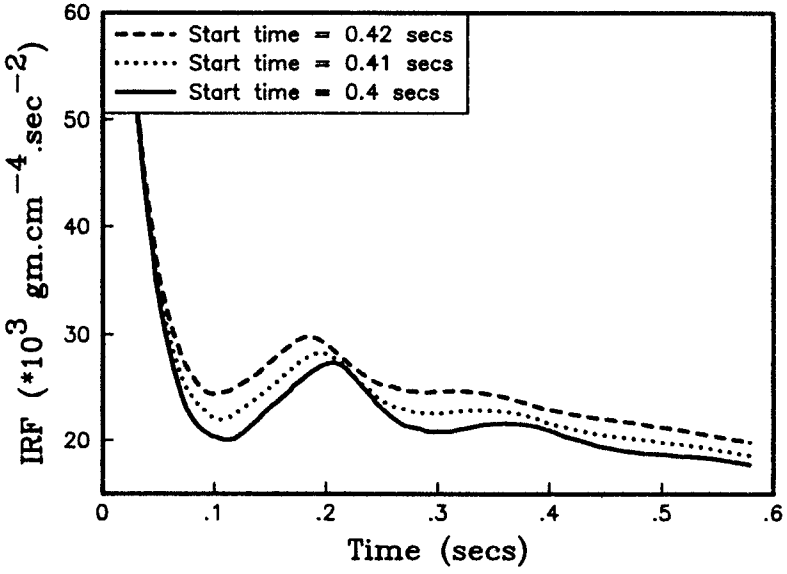

FIG (14)

Relationship between Alpha and Start time of deconvolution.

It was seen that as α increases, the optimum start times of deconvolution yeilding reliable estimates of compliance were found to decrease.

Fig (14a) shows the relationship between α and start time when the sample rate was 100/sec.

Fig (14b) shows the relationship between α and start time when the sample rate was increased to 256 samples/sec.

FIG (14a)

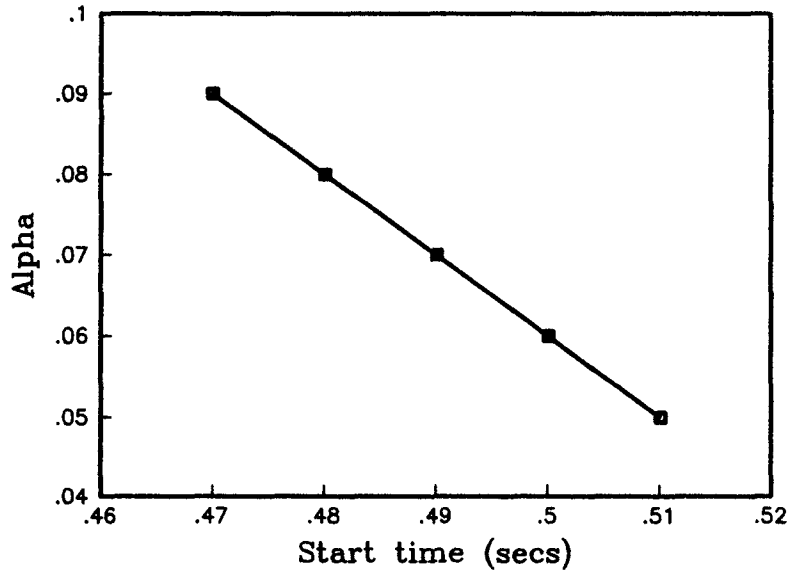

FIG (14b)

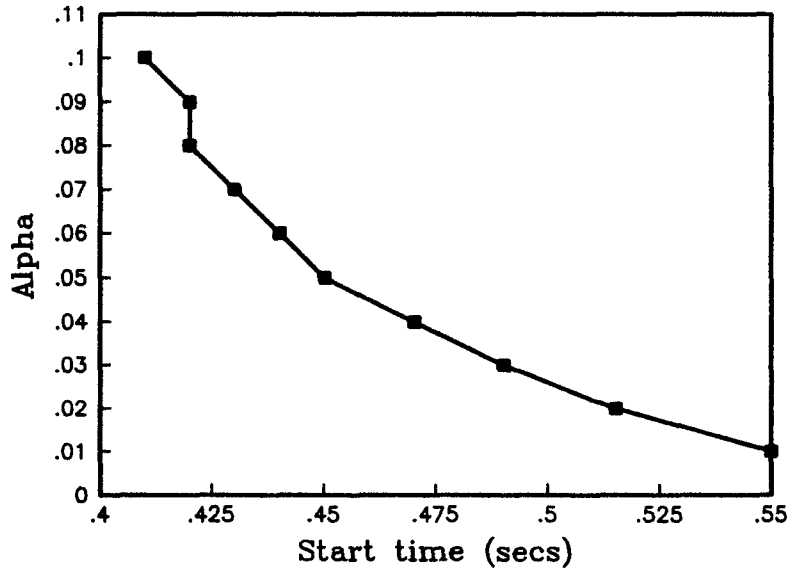

FIG (15)

Flow and pressure waveforms measured in dog1. The calculated hemodynamic parameters are

Peripheral Resistance : $R_p = 7.446\ (\times 10^3)\ gm.cm^{-4}.sec^{-1}$,

Capacitance : $C = 312\ (\times 10^{-6})\ gm^{-1}.cm^4.sec^2$

FIG (15)

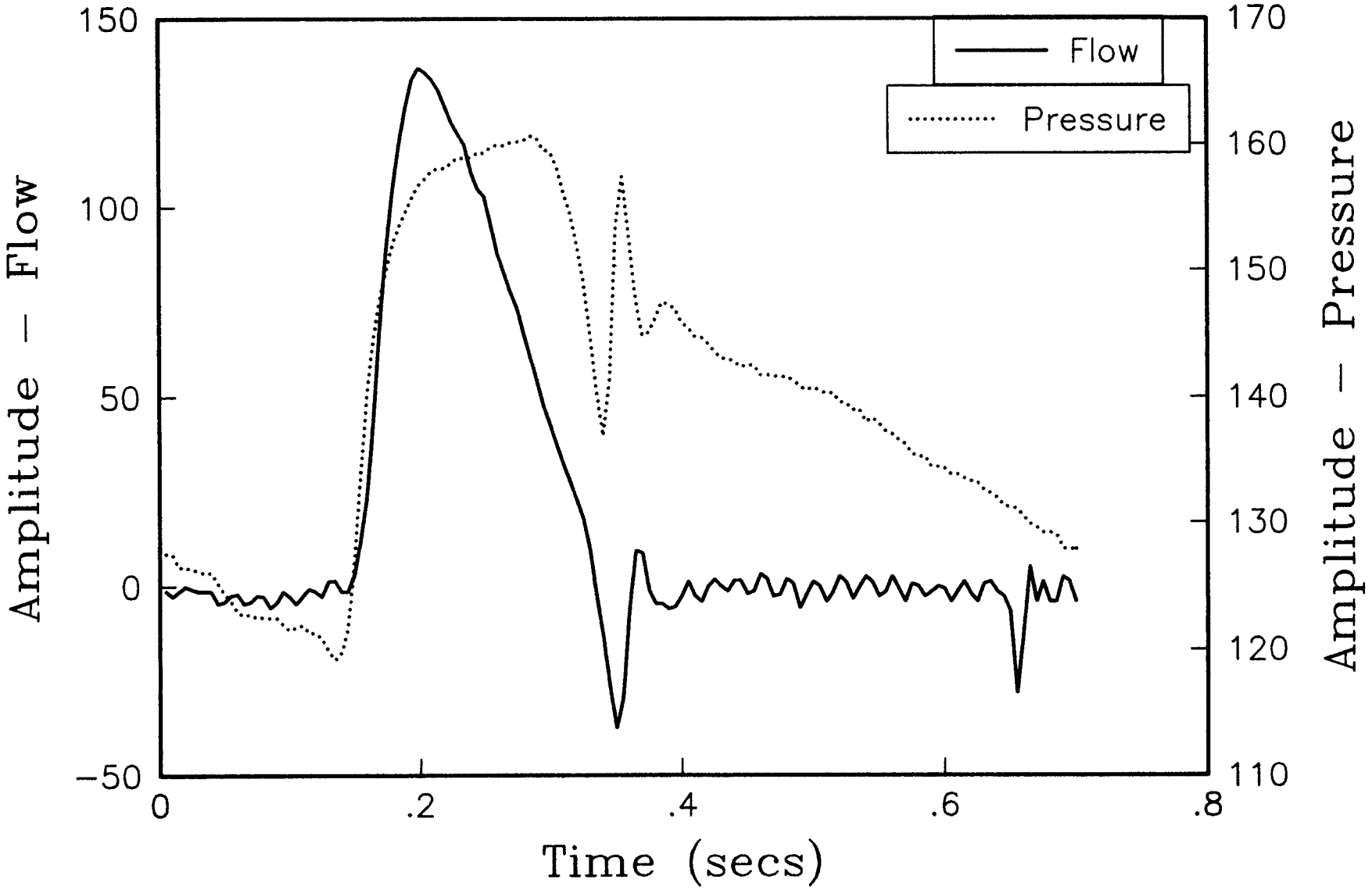
Flow
Pressure
150
100
50
0
−50
170
160
150
140
130
120
110
0
.2
.4
.6
.8
Amplitude – Flow
Amplitude – Pressure
Time (secs)

FIG (16)

Input Impedance of the arterial system computed from the pressure and flow data in doghr1, doghr2 & doghr3.

(Top : Modulus & Bottom : Phase in degrees)

FIG (16)

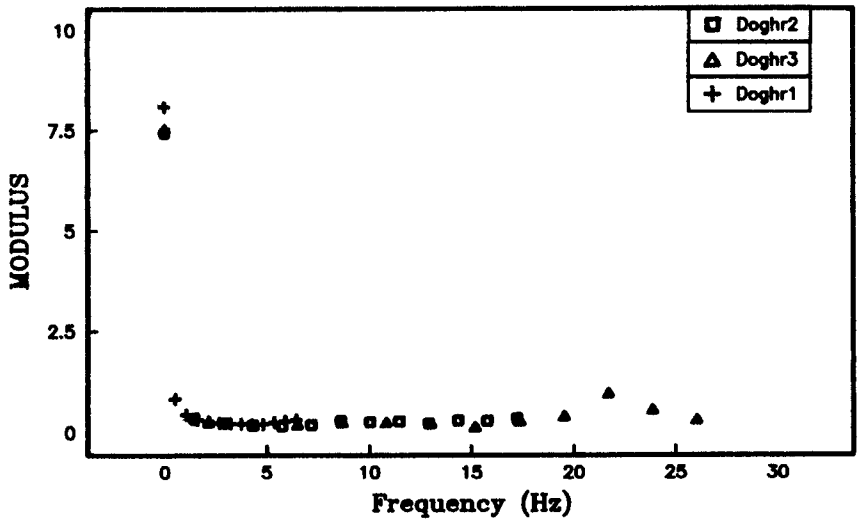
Doghr2
Doghr3
Doghr1
MODULUS
10
7.5
5
2.5
0
0
5
10
15
20
25
30
Frequency (Hz)

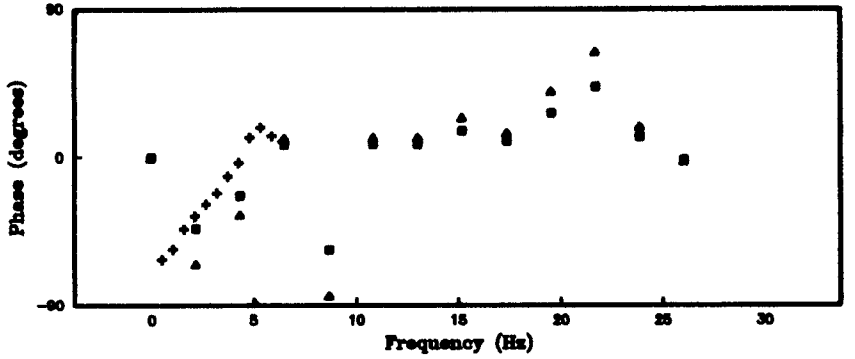
Phase (degrees)
90
0
-90
0
5
10
15
20
25
30
Frequency (Hz)

FIG (17)

The impulse response function of the arterial system of doghr2 computed by the transform method - Fig (17a).

The impulse response function of the arterial system of doghr3 - Fig (17b), computed by transform method.

The IRF of the arterial system of doghr1, computed by inverse Fourier transformation of the input impedance - Fig (17c).

FIG (17a)

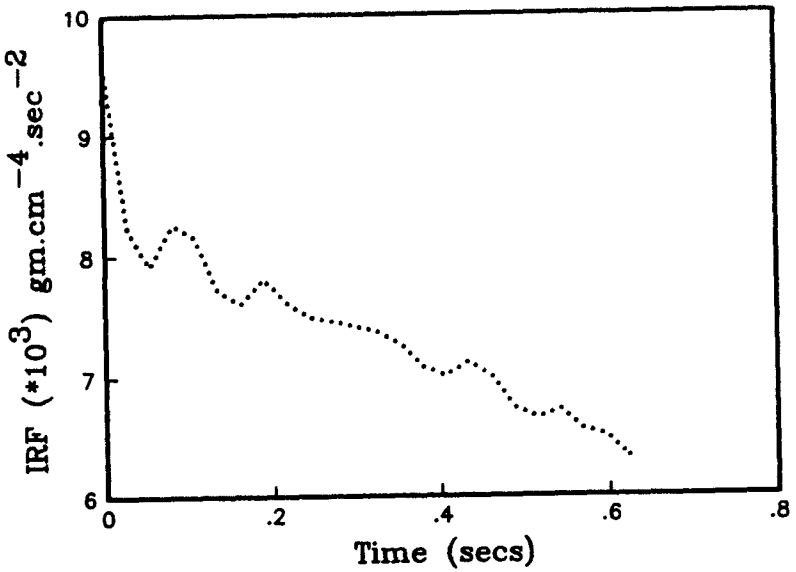

FIG (17b)

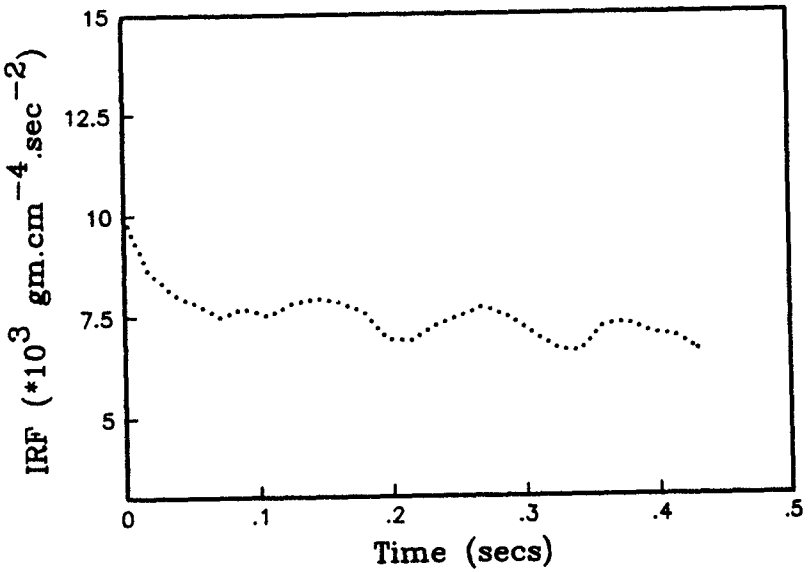

FIG (17c)

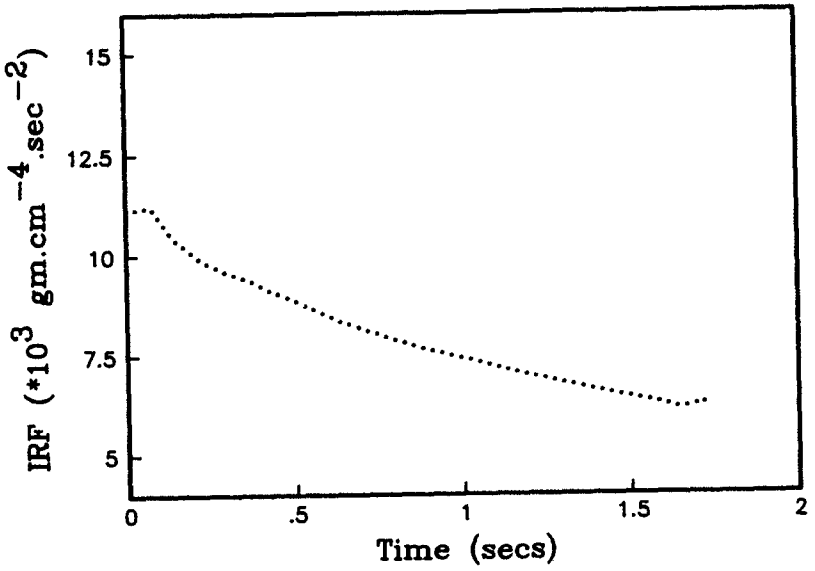

FIG (18)

Fig (18a) - The Impulse Response Function plots of the arterial system of doghr1 computed by Conventional method. The deconvolution was initiated at times t = 0.225 secs, 0.2 secs & 0.25 secs.
It was seen that this method resulted in incongruous IRF's.

Fig (18b) - Conventional method was used to compute the IRF of the arterial system of doghr2. It was computed for the following start times.
t = 0.2 secs
t = 0.225 secs
t = 0.25 secs

Fig (18c) - The IRF of the arterial system of doghr3 computed by the Conventional method.

FIG (18a)

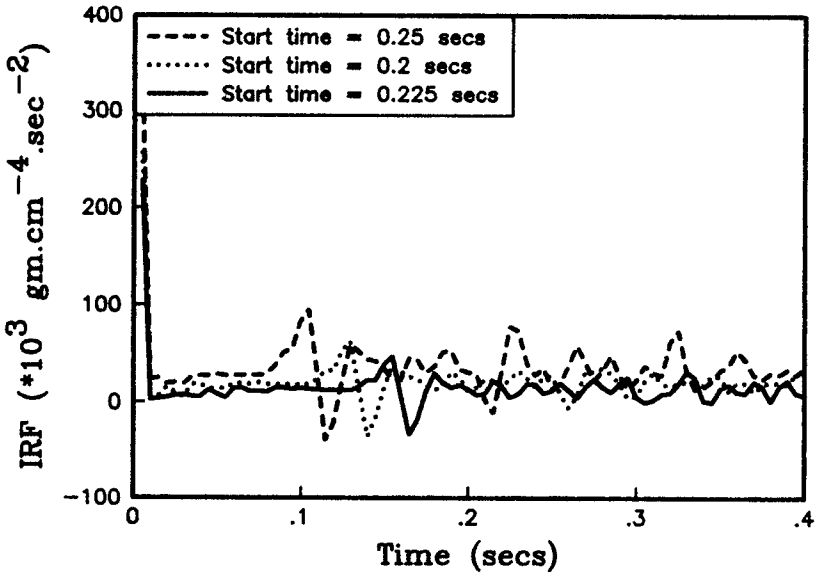

FIG (18b)

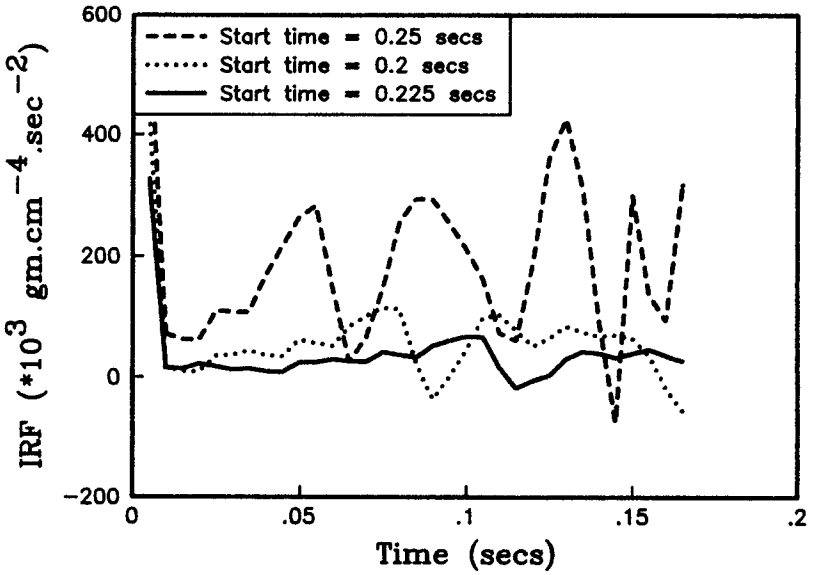

FIG (18c)

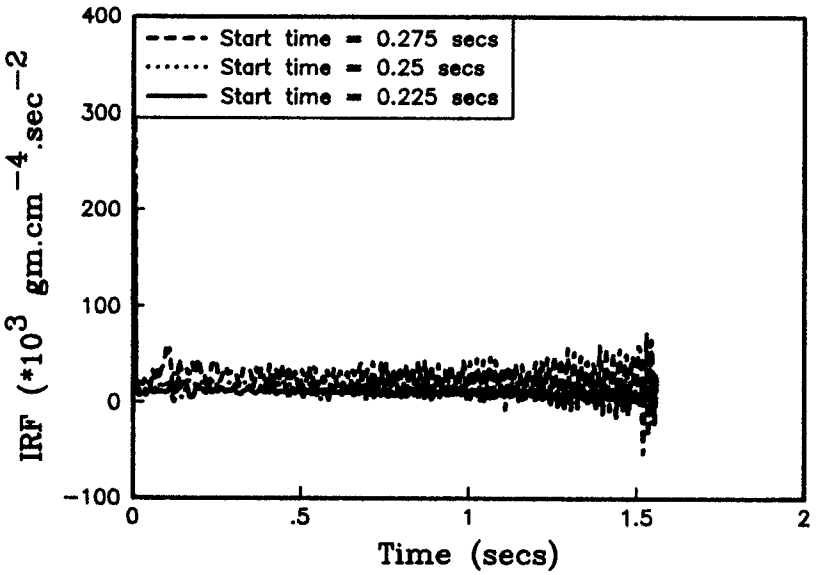

FIG (19)

The relaxation parameter was taken to be $\alpha = 1.0$ which reduces to the Gauss-Seidal method. This method was used to compute the IRF of the arterial system of doghr1 - Fig (19a).

The Gauss-Seidal method was used to compute the IRF of the arterial system of doghr2 - Fig (19b).

Using the Gauss-Seidal method, the impulse response function of the arterial system of doghr3 was calculated - Fig (19c).

This method proved futile in recovering the IRF from the flow and pressure data. for all three cases.

FIG (19c)

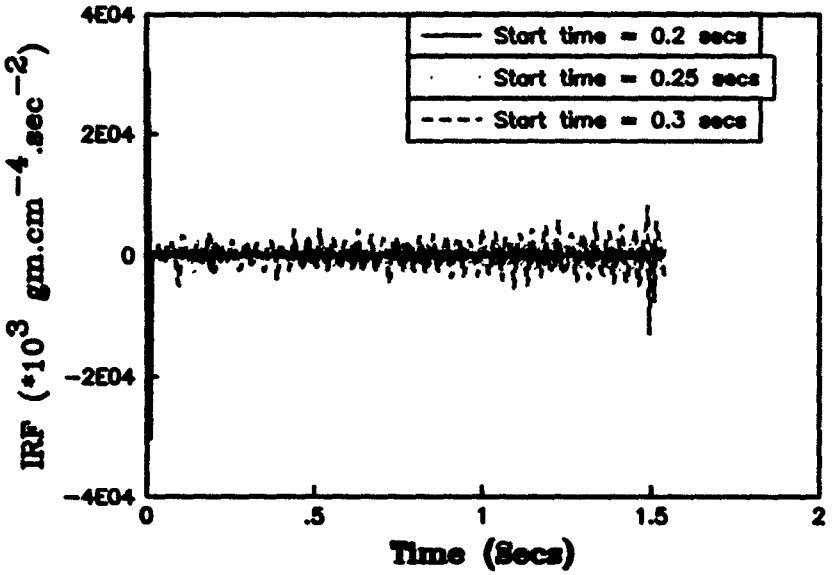

FIG (19a)

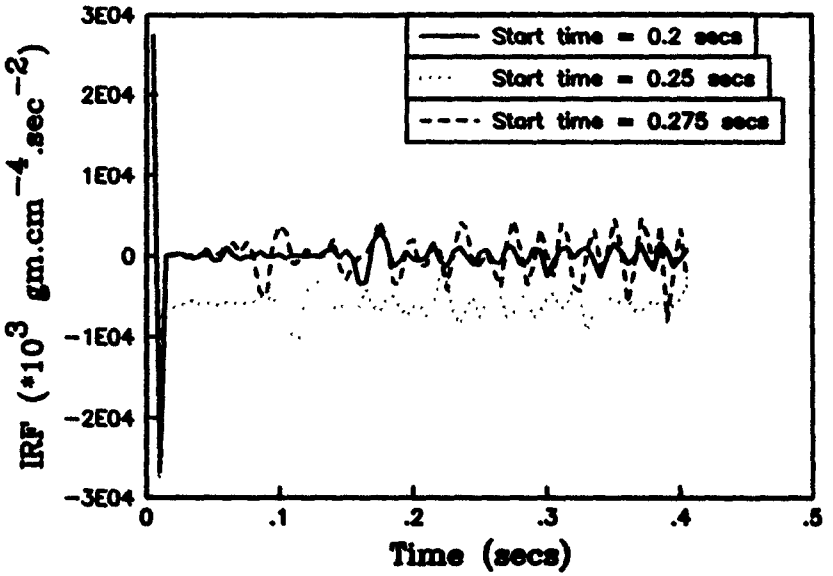

FIG (19b)

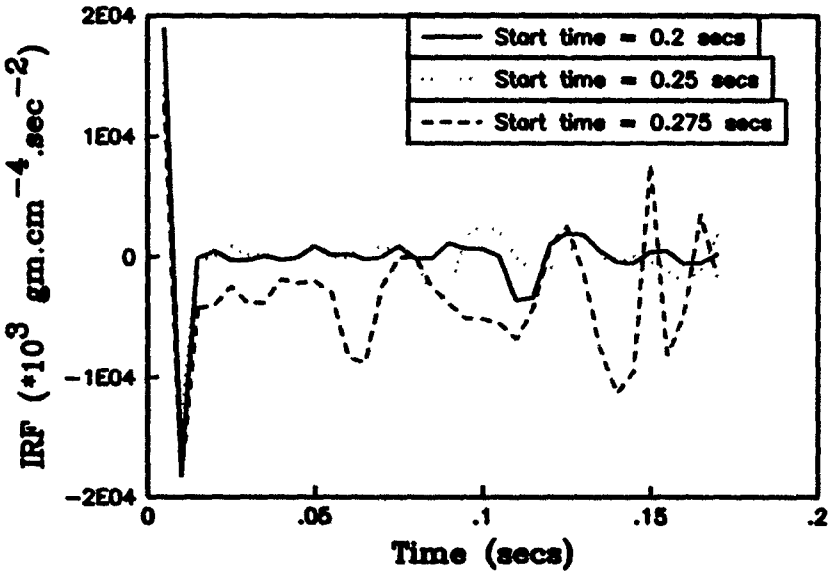

FIG (20)

The Over-relaxation method was then tried for all three cases under control conditions.

Fig (20a) - IRF plots of the arterial system of doghr1. The relaxation parameter taken to be 1.1 and different start times were tried. But it resulted in distorted IRF's.

Fig (20b) - The relaxation parameter was changed to 1.5 and deconvolution was initiated at the same start times.

Fig (20c) - IRF of the arterial system of doghr2 computed by the over-relaxation method with $\alpha = 1.1$.

Fig (20d) - IRF of the arterial system of doghr2 computed by the over-relaxation method with the relaxation parameter $\alpha = 1.5$.

FIG (20a)

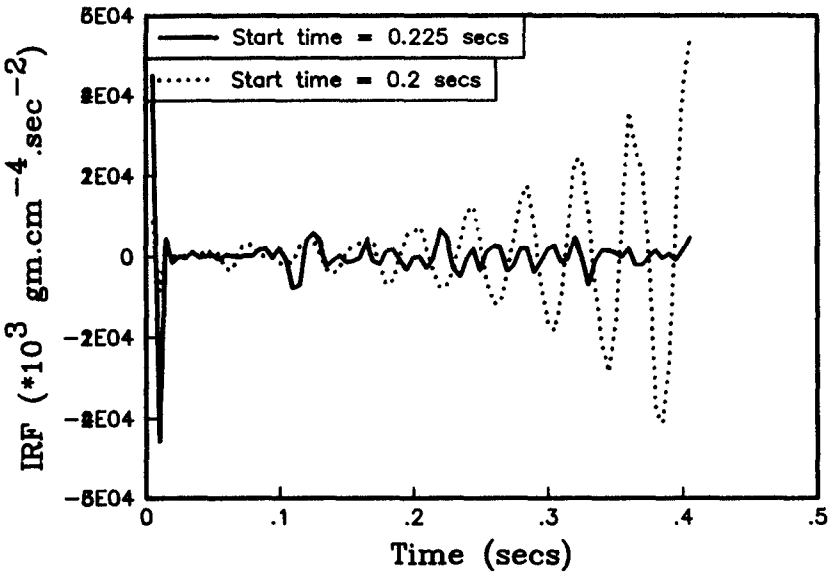

FIG (20b)

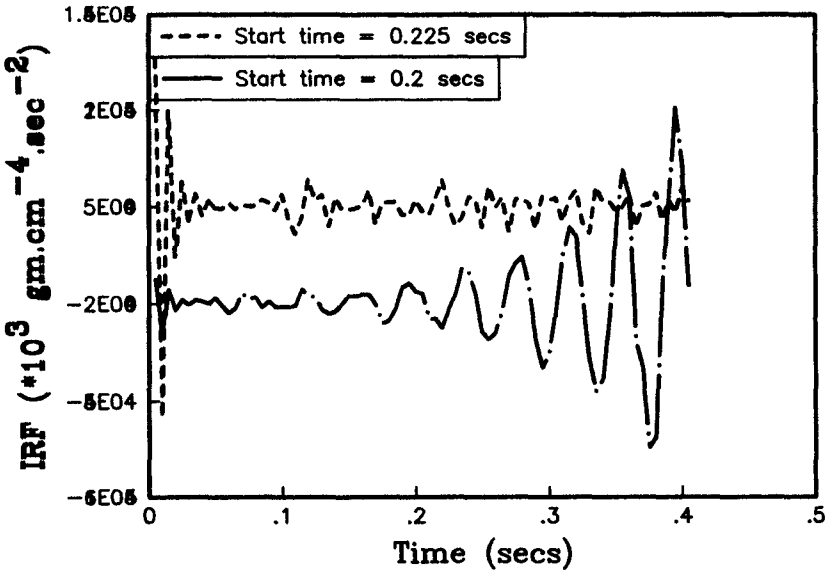

FIG (20c)

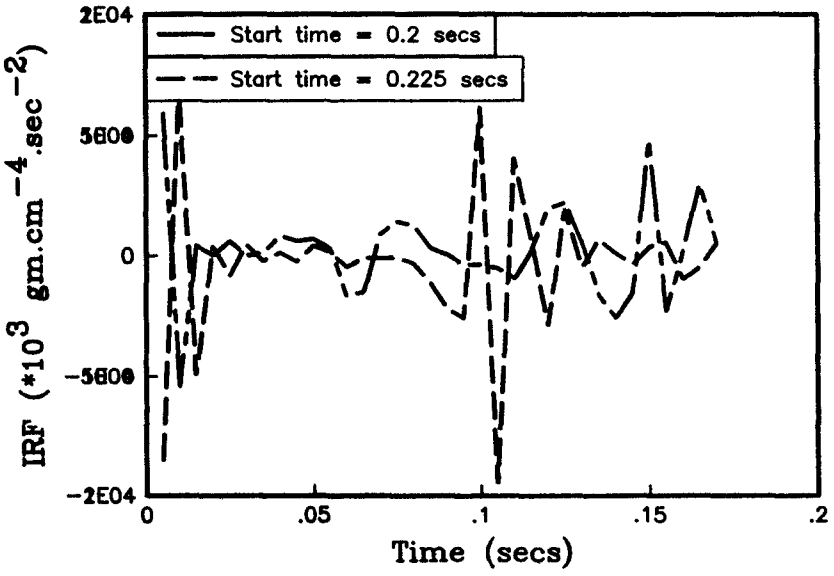

FIG (20d)

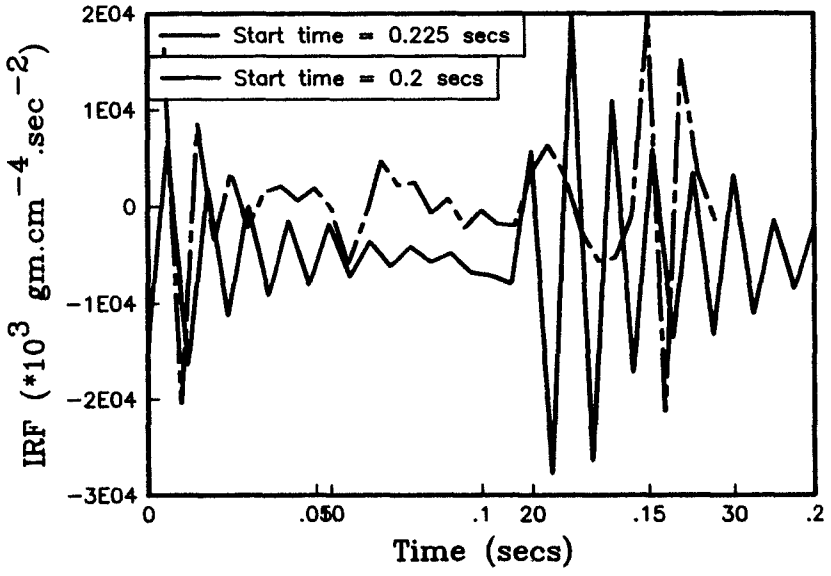

FIG (21)

IRF of the arterial system of doghr3 computed by the Over-relaxation method with $\alpha = 1.1$ & 1.5.

FIG (21a)

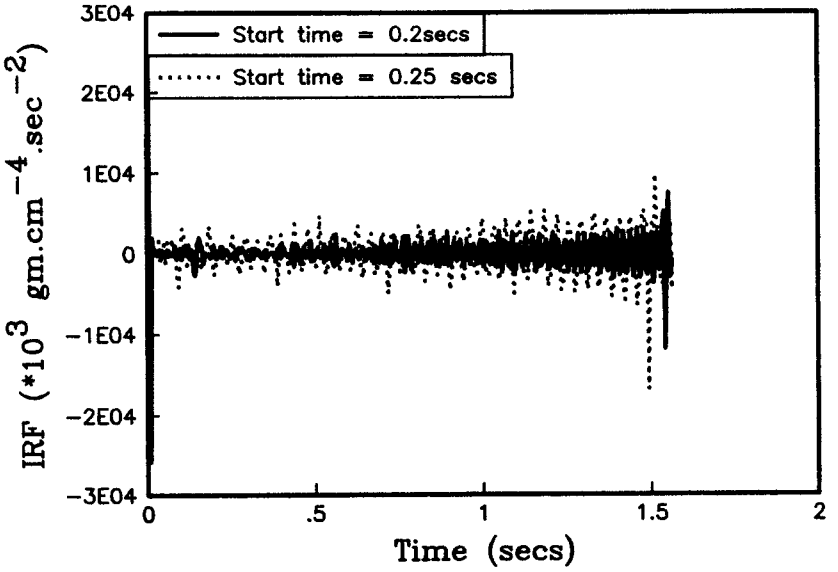

FIG (21b)

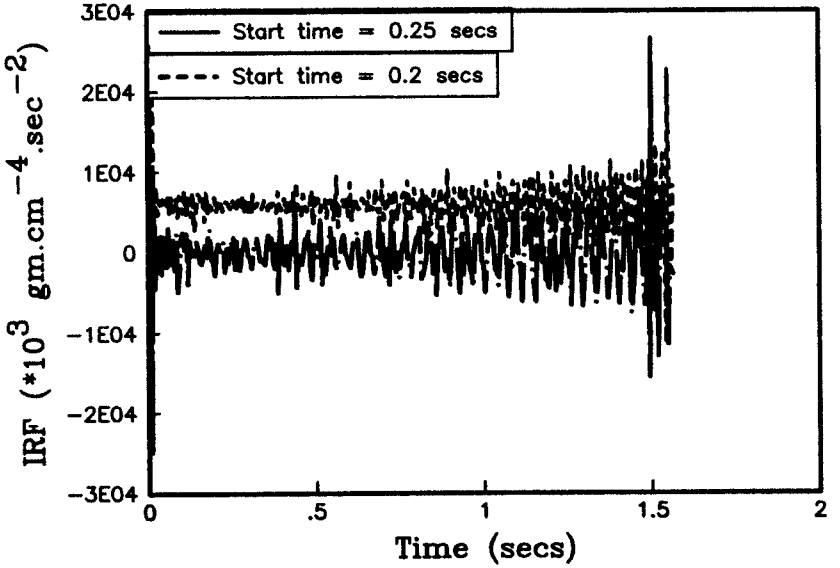

FIG (22)

Fig (22a) - IRF of the arterial system of doghr1. $\alpha = 0.01$.

Fig (22b) - IRF of the arterial system of doghr1. $\alpha = 0.02$.

Fig (22c) - IRF of the arterial system of doghr1. $\alpha = 0.03$.

FIG (22a)

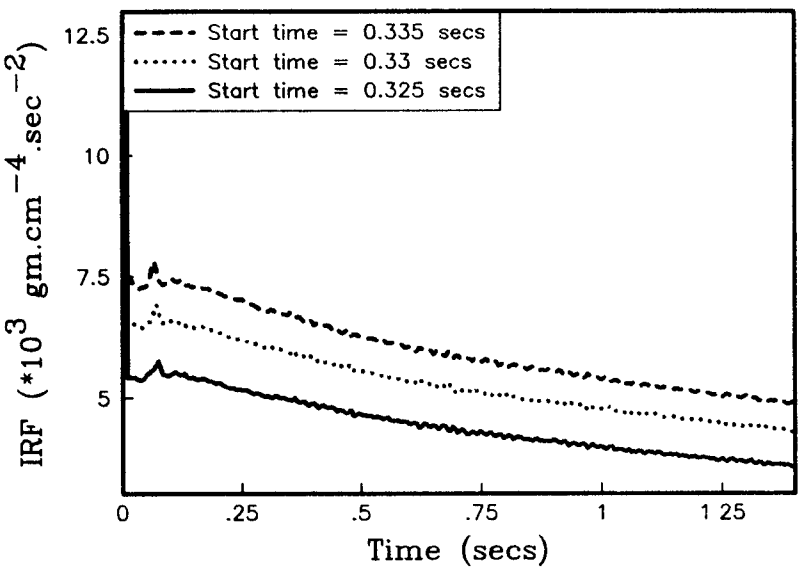

FIG (22b)

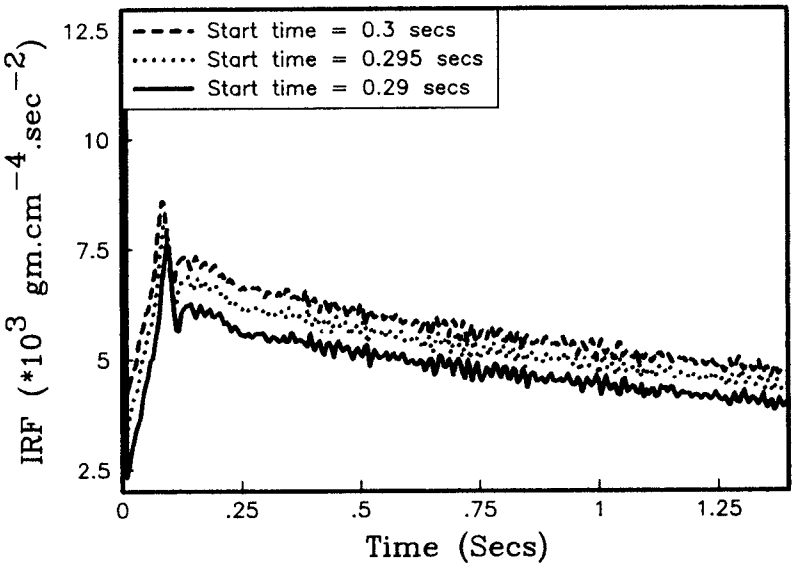

FIG (22c)

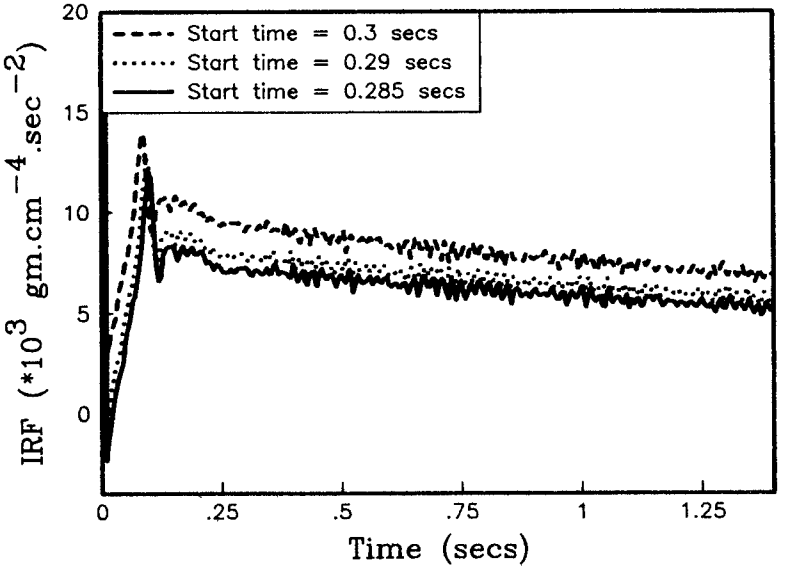

FIG (23)

The Under-Relaxation method was used to compute the IRF of the arterial system of doghr2.

Fig (23a) - The relaxation parameter α was taken to be 0.01. Different start times were investigated. The compliance value was estimated from the IRF plots. The compliance value which closely approximated the arterial compliance of doghr2 was obtained when the start time of deconvolution was 0.32 secs.

Fig (23b) - The IRF of the arterial system of doghr2 was computed by the Under-relaxation method with $\alpha = 0.02$. The start times of deconvolution used to compute the IRF are t = 0.3 secs, t = 0.305 secs and t = 0.31 secs.

The compliance values were estimated from the plots.

Fig (23c) - The value of α was set to be 0.03 and the impulse response

function of the arterial system of doghr2 was computed at various start times.

FIG (23a)

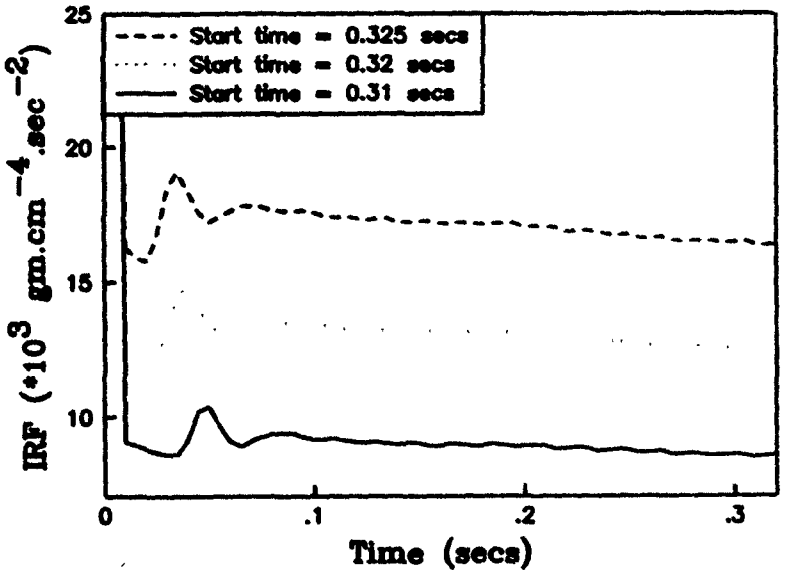

FIG (23b)

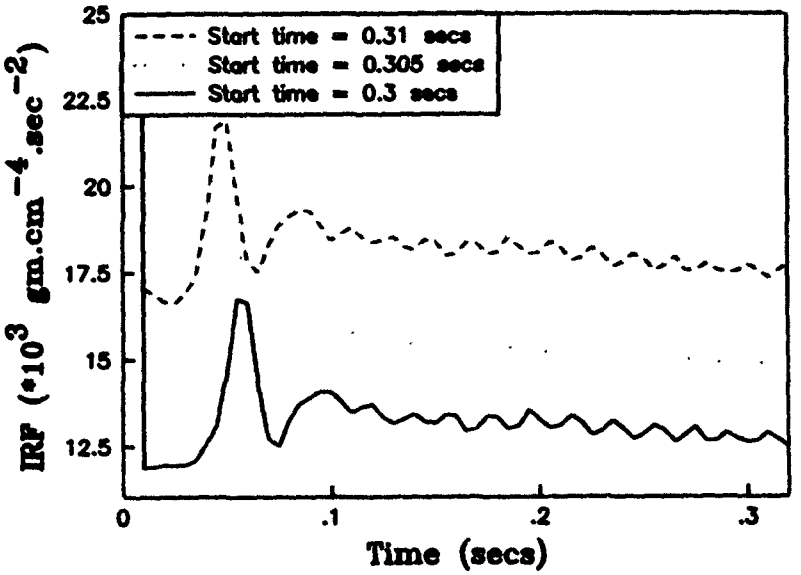

FIG (23c)

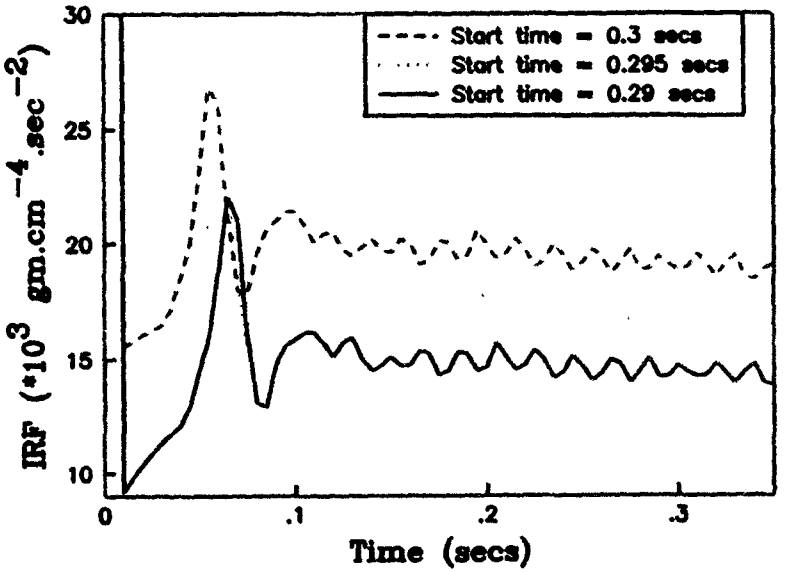

FIG (24)

The Under-Relaxation method was used to compute the arterial system of doghr3 with the relaxation parameter = 0.01 - Fig (24a). The start times considered were t = 0.275 secs , 0.28 secs & 0.29 secs.
The compliance values were estimated from the IRF plots. When deconvolution was initiated at 0.28 secs which corresponded to a start point of 56 samples, estimated compliance best approximated the total arterial compliance of doghr3.

The Under-relaxation method with α = 0.02 was used to compute the IRF of the arterial system of doghr3 - Fig (24b). The start time of deconvolution set to be 0.26 secs gave best results in terms of compliance.

The IRF of the arterial system of doghr3 computed when the relaxation parameter was = 0.03 - Fig (24c). The compliance values were estimated from the plots by extrapolating the exponential part of the IRF to time

FIG (24a)

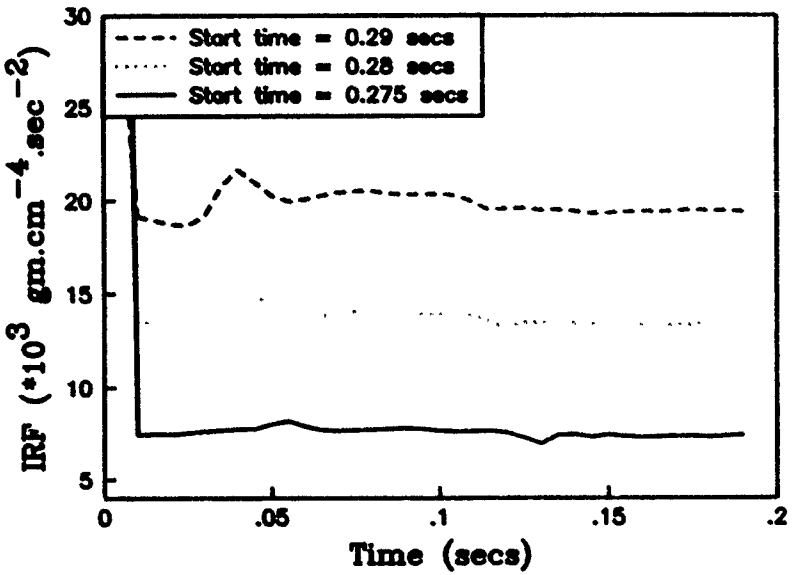

FIG (24b)

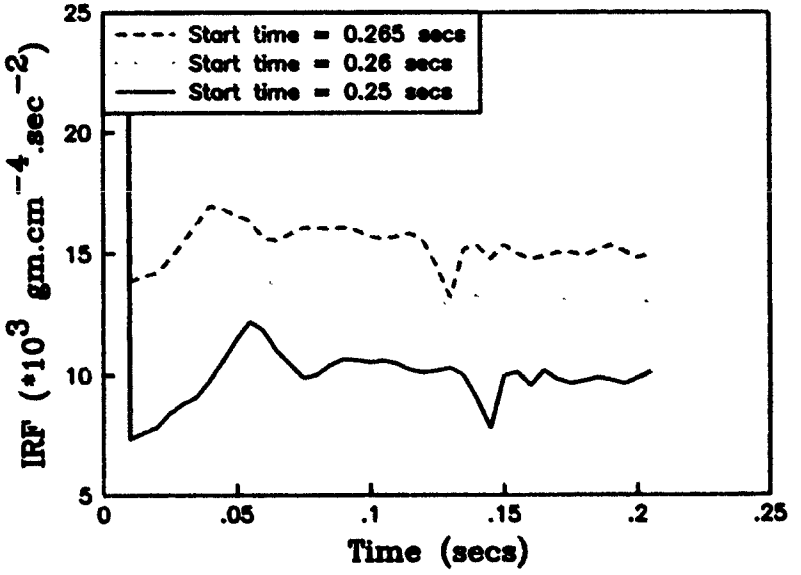

FIG (24c)

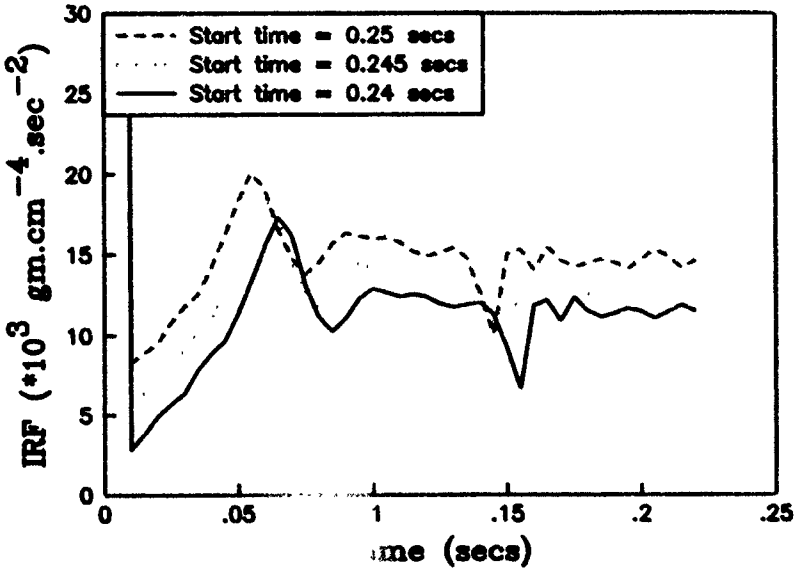

FIG (25)

Relationship of the relaxation parameter alpha with the start time of deconvolution. As α is increased, the optimum start times of deconvolution were found to decrease for all three cases.

Fig (25a)- Doghr1

Fig (25b) - Doghr2

Fig (25c) - Doghr3

FIG (25a)

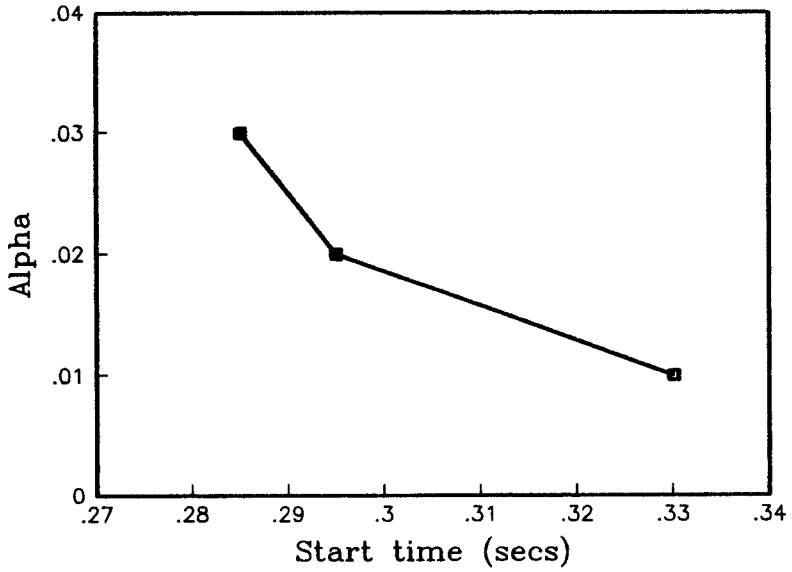

FIG (25b)

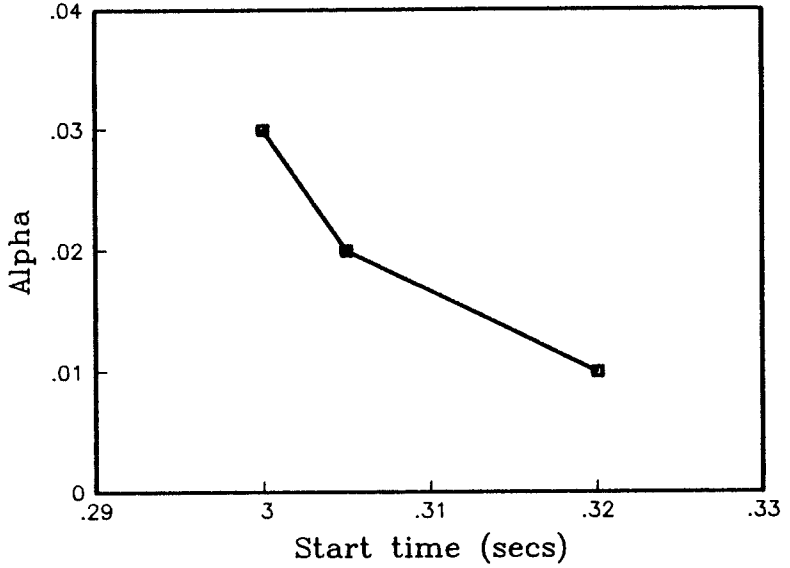

FIG (25c)

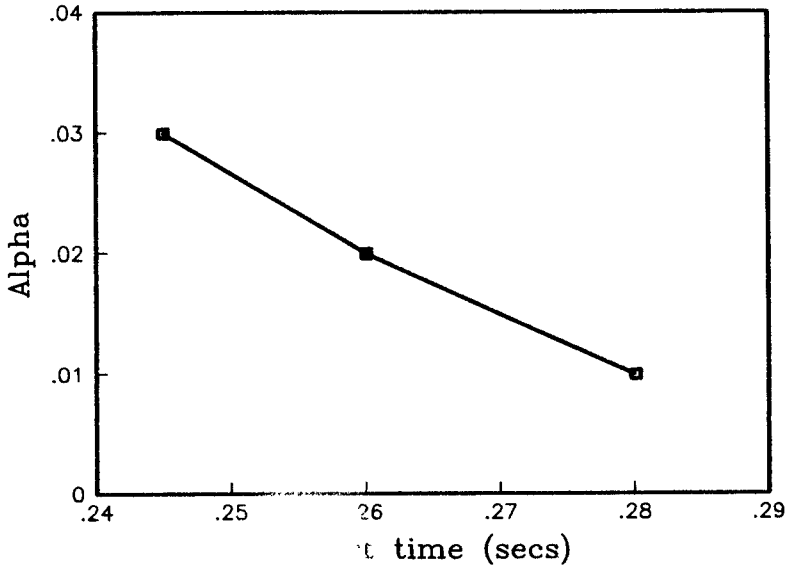

FIG (26)

Fig (26a) - Flow and Pressure waveforms in dog4. The calculated hemodynamic parameters for this dog are

Peripheral resistance : $R_p = 10.8\ (\times 10^3)\ gm.cm^{-4}.sec^{-2}$.

Capacitance : $C = 210\ (\times 10^{-6})\ gm^{-1}.cm^4.sec^2$.

Fig (26b) - Flow and pressure measured in dog5 - with occlusion of both carotid arteries. The hemodynamic parameters are

Peripheral Resistance : $R_p = 9.696\ (\times 10^3)\ gm^{-1}.cm^4.sec^2$.

Capacitance : $C = 322\ (\times 10^{-6})\ gm^{-1}.cm^4.sec^2$.

FIG (26a)

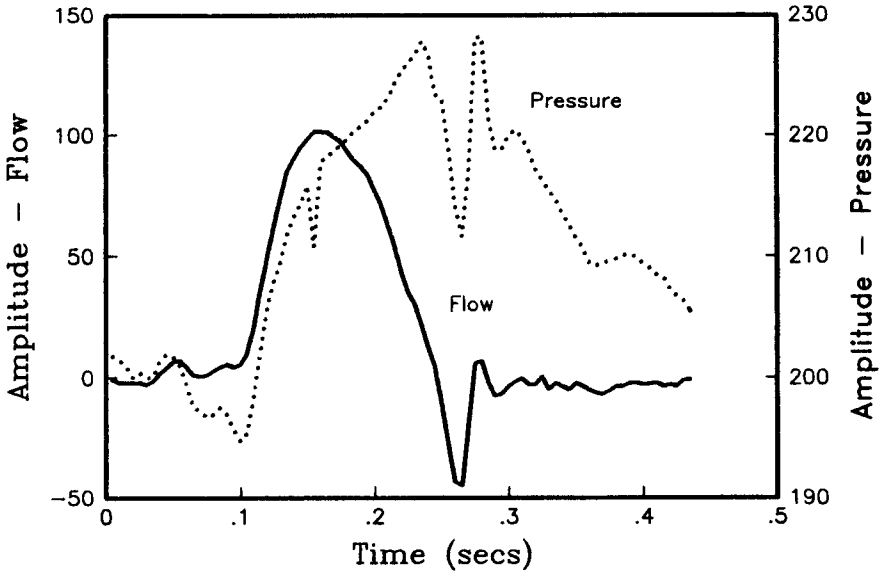

FIG (26b)

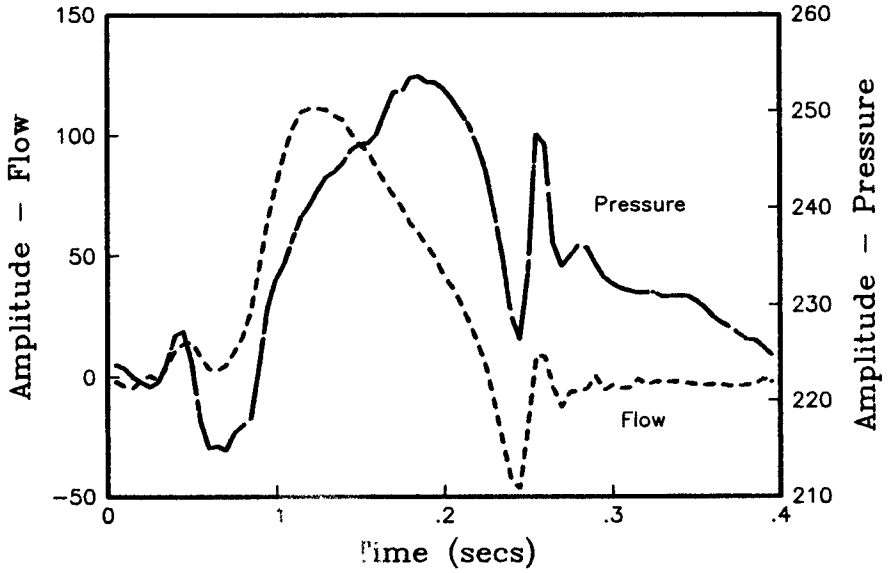

FIG (27)

Input impedance of the arterial system of dog4.

(Top : Modulus & Bottom : Phase in degrees).

FIG (27)

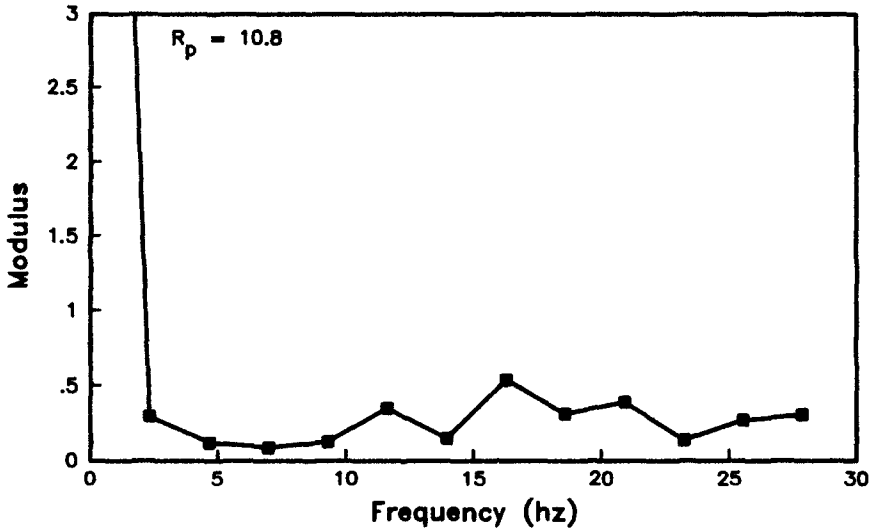

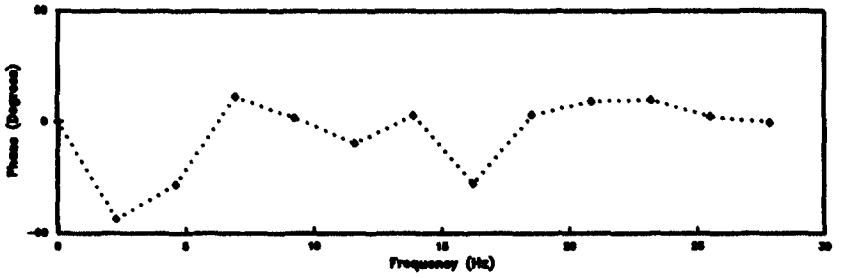

FIG (28)

Fig (28a) - Impulse response function of the arterial system of dog4 computed by the transform method.

Fig (28b) - IRF of the arterial system of dog5 computed by the transform method.

FIG (28a)

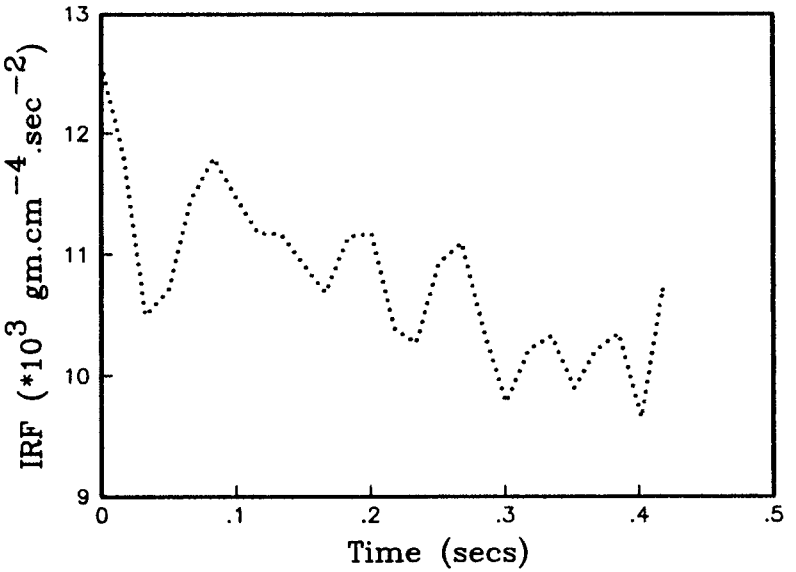

FIG (28b)

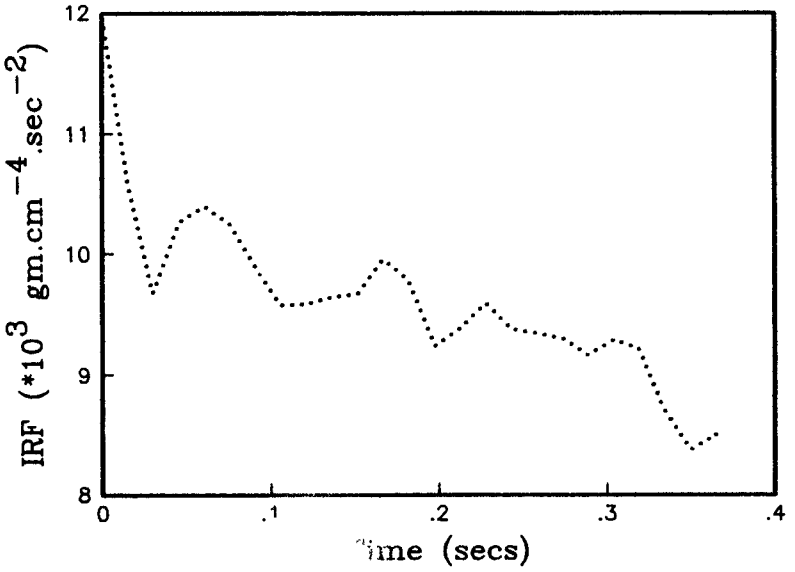

FIG (29)

Input Impedance of the arterial system of dog5 obtained from the pressure and flow data.

(Top : Modulus & Bottom : Phase in degrees).

FIG (29)

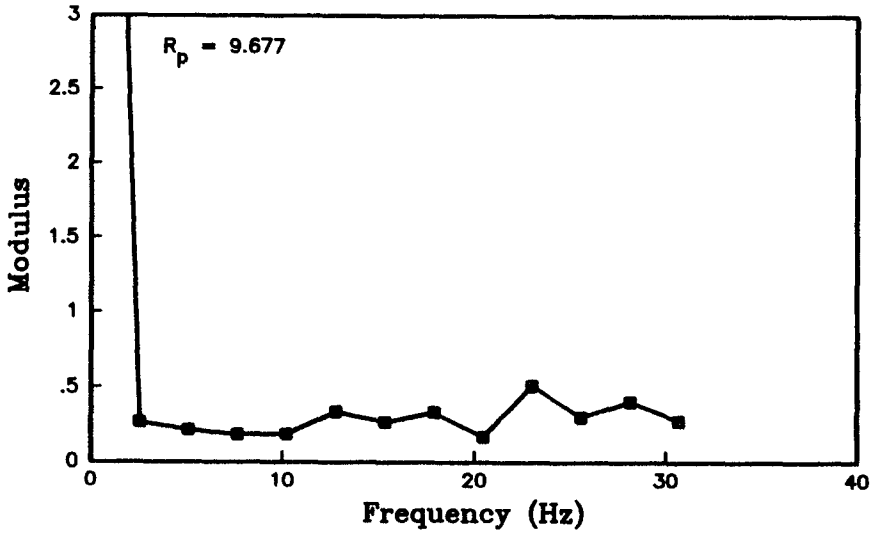
R_p = 9.677
Modulus
3
2.5
2
1.5
1
.5
0
0
10
20
30
40
Frequency (Hz)

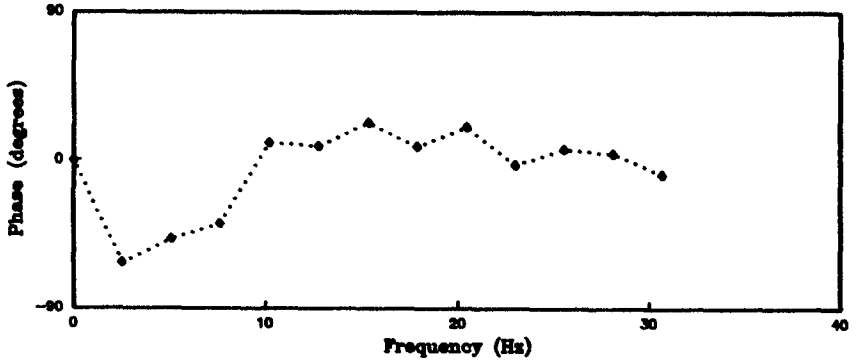
Phase (degrees)
90
0
-90
0
10
20
30
40
Frequency (Hz)

FIG (30)

Fig (30a) & Fig (30b) - IRF of the arterial system of dog5 calculated using the Conventional method.

FIG (30a)

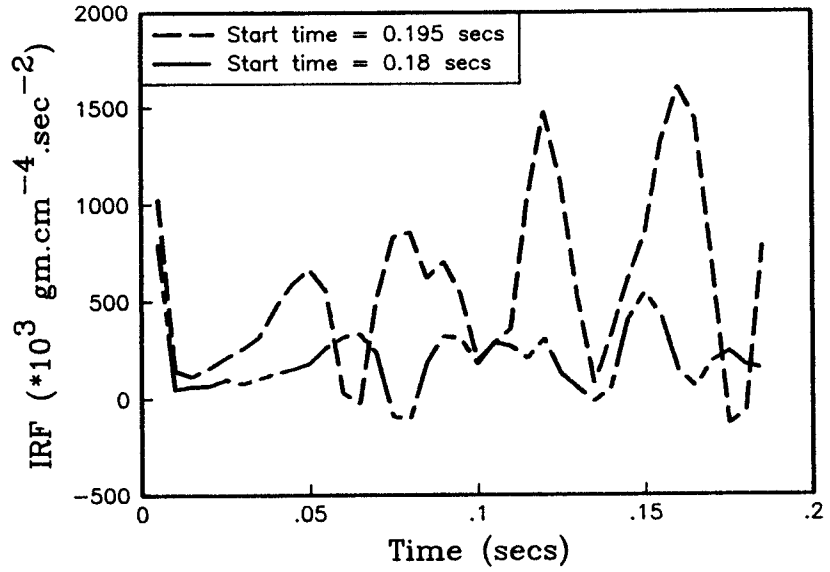

FIG (30b)

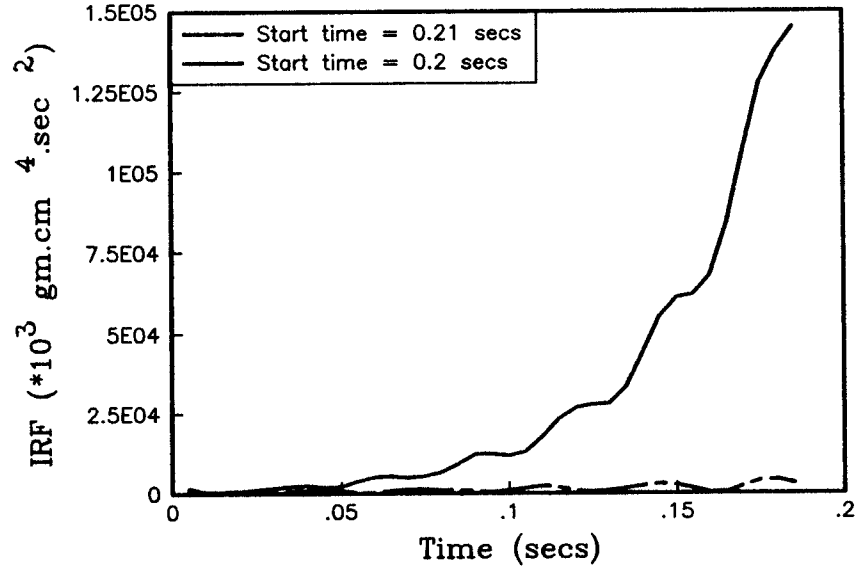

FIG (31)

Fig (31a) - The Gauss-Seidal method was used to calculate the IRF of the arterial system of dog5. The relaxation parameter $\alpha = 1.0$.

Fig (31b) - The Over-relaxation method was used to compute the IRF of dog5. The relaxation parameter was chosen to be 1.1 & 1.5. Different start times were tried.

FIG (31a)

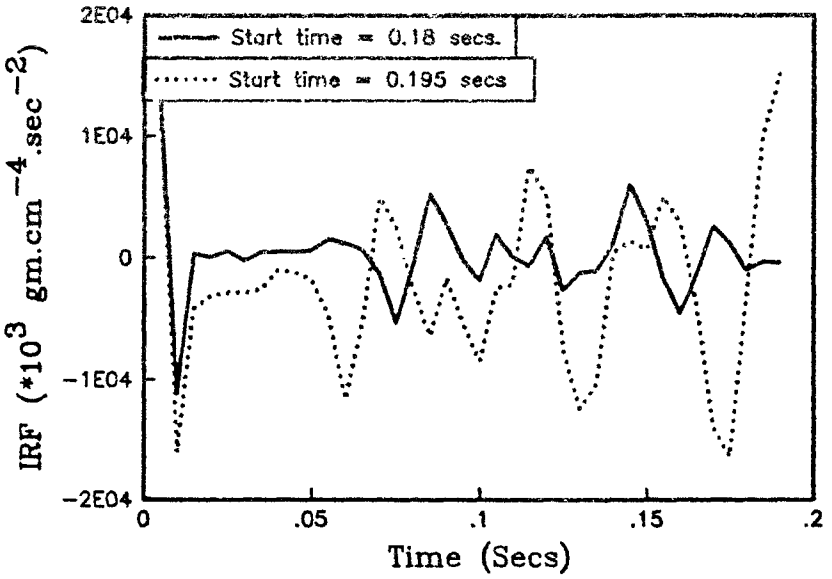

FIG (31b)

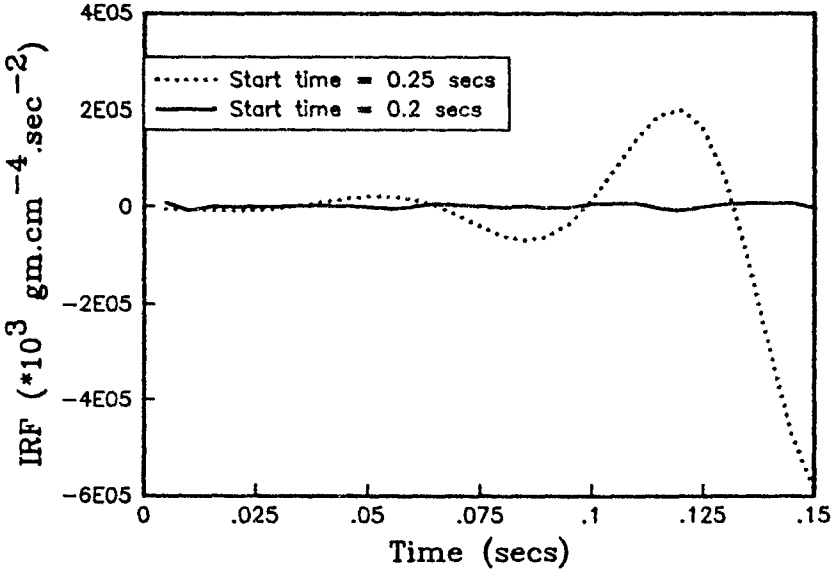

FIG (32)

The Under-relaxation method with α equal to 0.01 was applied to the data from dog5.

Fig (32a) - Start time = 0.21 secs.

Fig (32b) - Start time = 0.215 secs.

FIG (32a)

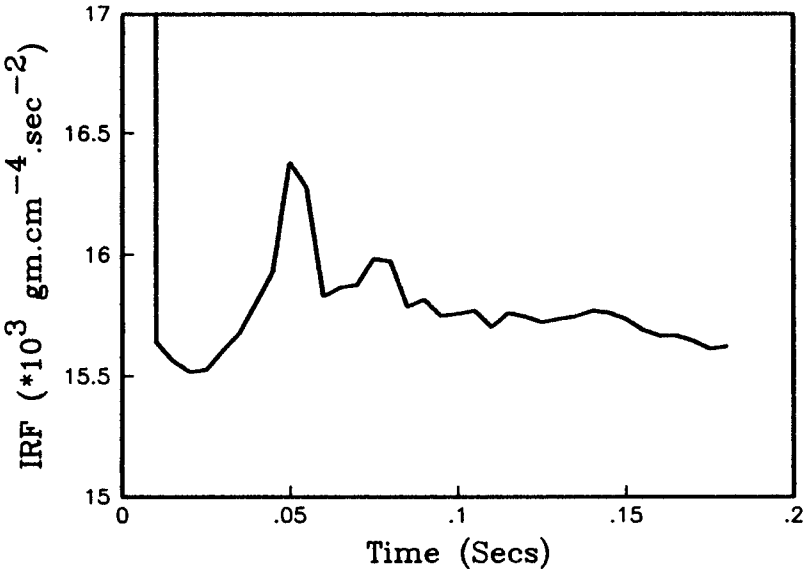

FIG (32b)

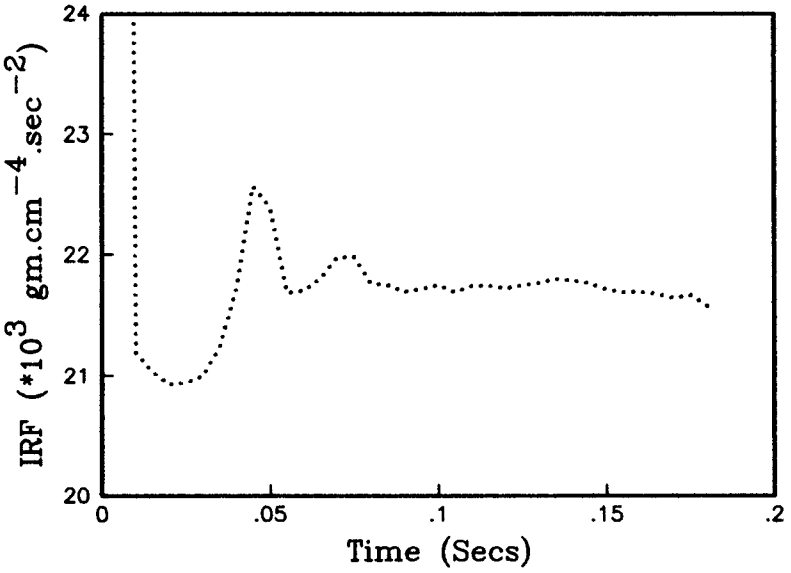

FIG (33)

The Under-relaxation method was applied to the flow and pressure data of dog5 with the relaxation parameter set to be 0.02.

Fig (33a) - The start time was set to be 0.18 secs.

Fig (33b) - The start time was equal to 0.19 secs.

Fig (33c) - The start time was set equal to 0.195 secs which gave best estimates of compliance.

FIG (33a)

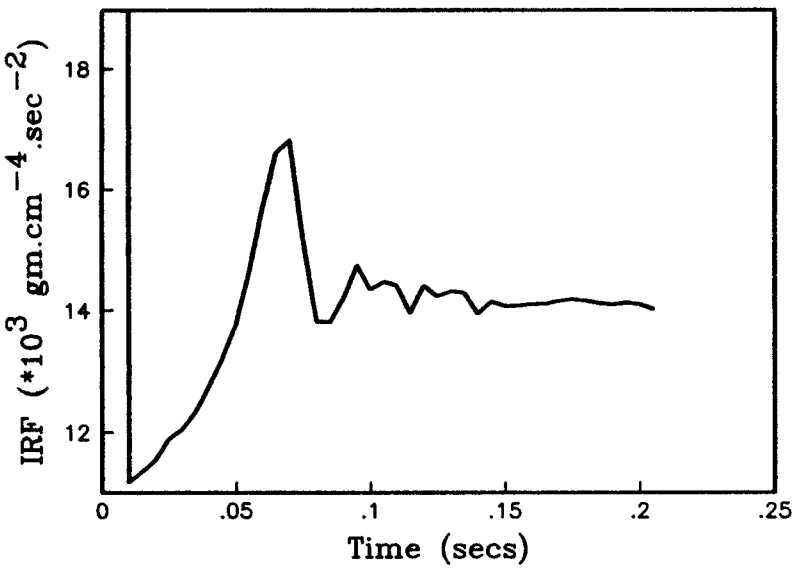

FIG (33b)

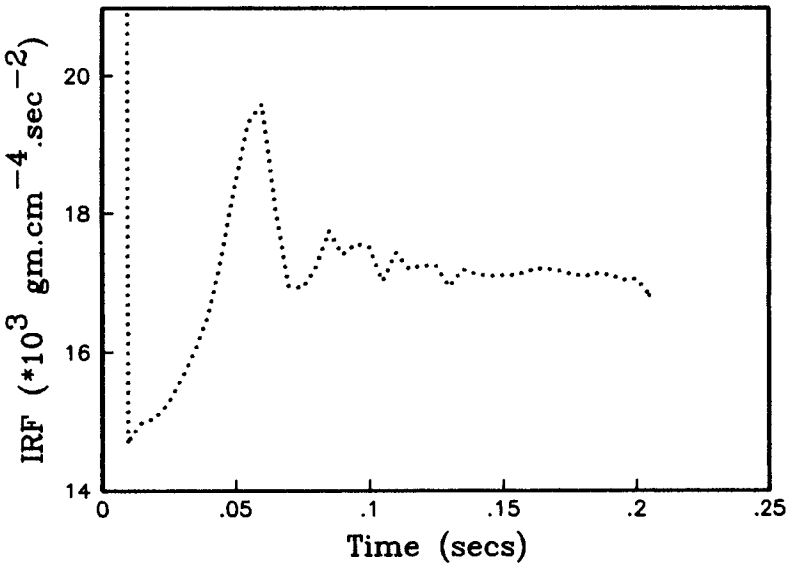

FIG (33c)

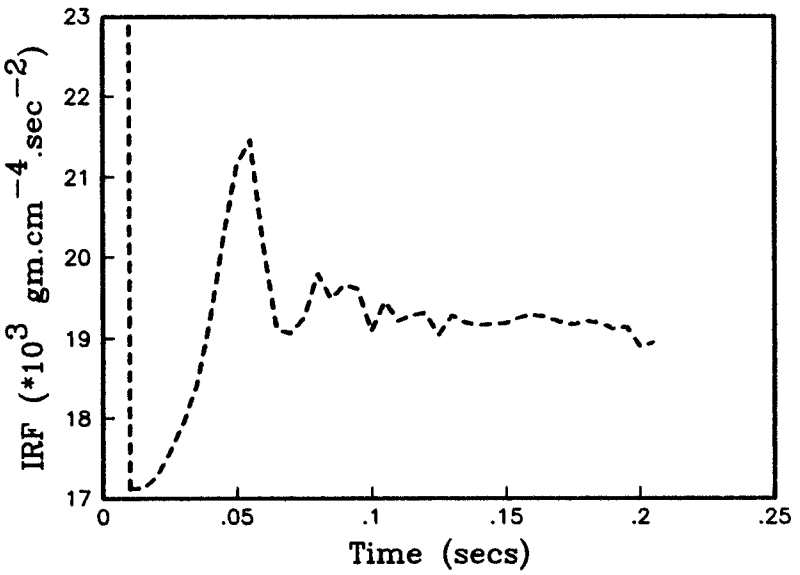

FIG (34)

Relationship between α and the start time for dog5.

FIG (34)